3

Analytical Application of Single-Photon Ionization Mass Spectrometry (SPI-MS)

Thorsten Streibel[1,2], *Hendryk Czech*[1,2], *and Ralf Zimmermann*[1,2]

[1] *University of Rostock, Institute of Chemistry, Joint Mass Spectrometry Centre (JMSC) of Rostock and Helmholtz Zentrum München; Chair of Analytical Chemistry, Dr.-Lorenz-Weg 2, D-18051 Rostock, Germany*
[2] *Research Unit "Comprehensive Molecular Analytics" – CMA, Helmholtz Zentrum München – German Research Center for Environmental Health GmbH, Gmunder Str. 37, D-81379 München, Germany*

Single-photon ionization (SPI), using vacuum ultraviolet light (VUV) for soft, low fragmentation ionization of organic compounds, is increasingly applied as a versatile ionization method in analytical mass spectrometry. While the fundamentals of SPI are considered in Chapter 1, this chapter is focusing on the application of SPI-MS in analytical chemistry. Firstly, an overview on the different light sources for the generation of vacuum-ultraviolet (VUV) light, both lamp and laser based, is given. Afterwards, a broad survey of applications from various fields, utilizing VUV light for mass spectrometric analysis of organic trace species is provided. This ranges from direct SPI-MS process gas analysis or combustion effluent on-line monitoring applications via the utilization of hyphenated systems, such as gas chromatography-SPI-MS, to ambient monitoring solutions. Finally, existing commercial systems are briefly presented.

3.1 VUV Light Sources

Sources for the generation of VUV light can be roughly divided into two categories. Firstly, VUV light can be produced by lamp-based sources, which deliver incoherent VUV light beams mostly in a continuous way. Secondly, pulsed VUV beams can also be generated by laser sources, e.g. by frequency tripling in rare gas mixtures. The fluorine excimer laser provides a unique source for pulsed VUV radiation with a wavelength of 157 nm without the need of frequency multiplication. Finally, the utilization of synchrotron radiation constitutes an additional possibility for producing VUV light with the advantage to get the radiation easily in a tunable manner, however requiring a greater effort in the design of the experimental setup at large synchrotron facilities. This makes on-site applications impossible. Synchrotron radiation is produced when charged electrons are accelerated perpendicularly to their direction of propagation. It exhibits some unique properties valuable for VUV generation,

Photoionization and Photo-Induced Processes in Mass Spectrometry: Fundamentals and Applications,
First Edition. Edited by Ralf Zimmermann and Luke Hanley.

such as yielding a broad spectrum covering a range between 70 and 200 nm, high flux and brilliance, polarization, and pulsed time structure (Qi et al. 2006; Qi 2013). Electron storage rings with bend magnets are a common device for the generation of synchrotron radiation by providing a radial acceleration to the electrons, which have kinetic energies of approximately 1 GeV. The subsequently generated synchrotron radiation therefore can be seen as a special form of bremsstrahlung. Undulators are a special periodical structured configuration of magnets, which forces entering electrons into oscillations, causing them to emit synchrotron radiation in the average direction of their flight path. Despite the broad wavelength distribution of the emitted synchrotron radiation, selection of distinct photon energies is quite easy, yielding in a versatile, tunable VUV source with high energy resolution. Monochromator gratings cut out the desired wavelength range (for VUV radiation 70–200 nm) with an energy resolution ($E/\Delta E$) up to 1000. In Chapter 5, the applications of synchrotron VUV radiation in photoionization mass spectrometry are described in more detail.

3.2 Lamp-Based VUV Light Sources

Discharge lamps provide a convenient for the generation of VUV light. The most common execution of this principle are low-pressure rare gas discharge lamps. The gases contained in sealed lamps are excited by a glow discharge, producing spectral emission lines (i.e. atomic transitions) down to short wavelengths in the VUV range. Such lamps emit VUV radiation with high spectral and intensity stability. The VUV radiation is then emitted through magnesium fluoride (MgF_2) or lithium fluoride (LiF) windows. Lamps can be operated with either direct current voltage or radio frequency-powered fields in the MHz region. Different wavelengths are available, depending on the applied rare gas. With xenon, 129 and 147 nm emission lines are emitted equivalent to 9.6 and 8.4 eV, respectively. Krypton yields 117 and 124 nm light (10.6 and 10.0 eV), whereas with argon even a wavelength as short as 105 nm is accessible (11.8 eV). For those high-energy VUV photons, however, LiF windows are necessary because they lie below the frequency cutoff of MgF_2. Such low-pressure discharge lamps are widely available commercially and are often referred to as photoionization detector (PID) lamps.

The efficiency of VUV lamps as photoionization sources for mass spectrometric applications can be enhanced by coating the repeller and focusing electrodes with a VUV reflecting material such as aluminum. Back-and-forth reflection of the VUV photons inside the ion source of a time-of-flight mass spectrometer increases the signal strength of the mass spectrometric detection (Zhu et al. 2014).

Another easily accessible VUV source is provided by deuterium arc lamps. They operate by creating an arc between a tungsten filament and a ceramic or metal anode and require preheating. The lamps are filled with low-pressure molecular deuterium, which is excited by the arc discharge and yields a broad emission spectrum ranging from 112 to 900 nm with especially intense continuum radiation in the UV- and VUV-range (emission from excited

dissociative D2 molecular states and molecular-recombination emission of deuterium atoms from previously dissociated D2 molecules). Again, an MgF_2 window is used for coupling out VUV light.

Excimer lamps using microdischarges with gas mixtures of rare gases and halogens under elevated pressures (900 mbar) have also been described. Powered by a radio frequency field, they yield brilliant VUV radiation of 193 nm when using a mixture of argon and 0.6% fluorine in helium or 157 nm when using 1% F_2 in helium (Salvermoser and Murnick 2004). The source of the radiation is hereby based on the decay of excited dimers (i.e. so called excimers), which is described in more detail below.

Another fundamental principle that can be applied to produce VUV radiation is the dielectric barrier discharge, where the electrical discharge takes place between two electrodes that are separated by a dielectric barrier. Krypton is used as a discharge gas; and upon its excitation to high levels, it achieves intense discharges that are distributed in space and time, and molecule formation occurs in the afterglow of these discharges (Ren'an et al. 2012).

An alternative way for rare gas excimer formation is the microhollow cathode discharge, in which a glow discharge can be operated at high density by confining the discharge current to narrow channels in a dielectric material. A disadvantage of such lamps are the erosion processes of the electrodes, leading to impurities. Also with inductively coupled microplasma, it is possible to generate VUV radiation. After ignition of a helium plasma under atmospheric conditions, VUV radiation from nitrogen and oxygen could be extracted. The source is available in a miniaturized device on a chip generating a microplasma of 200 µm diameter (Sato et al. 2014).

Brilliant electron beam-pumped excimer VUV light sources have been developed and applied with the purpose of on-line characterization of complex mixtures in mind. These excimer light sources use an electron beam to excite the rare gases. The special innovation of such light sources lies in a $0.7 \times 0.7\ m^2$, 300 nm thin silicon nitride foil, which separates the vacuum chamber containing the electron source from the section including the rare gas. The electron source generates an electron beam of 13–15 keV, which is guided through the foil exhibiting almost no loss of energy. When penetrating into the dense rare gas with a pressure of 1–2 bar, the electrons excite and partially ionize the rare gas atoms, leading to the formation of excited diatomic rare gas molecules (excimers). Upon the radiative decay of these excimers, intense VUV radiation is generated. Therefore, the formation of the excimers is restricted to a small volume element immediately behind the foil, resulting in a light beam of high brilliance. The beam is collected, focused, and coupled out by an MgF_2 lens system, which collects approximately 1–2% of the VUV light, resulting in a photon density in the order of magnitude of 10^{13} VUV photons per second (Morozov 2008; Mühlberger 2002). Such lamps are also eligible for pulsed operation with up to kHz repetition rates, yielding photon emissions of up to 10^{16} photons per second.

There also exists a possibility to produce emission of VUV light with narrow bandwidths of <0.1 nm with electron beam-pumped excimer lamps. If a small portion of hydrogen is added to neon, VUV emission at the position of the Lyman-α transition of hydrogen (121.6 nm) is accessible. One drawback of this

kind of electron-beam pumped VUV light source is the relatively fragile silicon nitride foil which easily breaks, e.g., when higher electron beam intensities are applied. This may limit the obtainable intensity of the emitted VUV light and the ruggedness of the light source for some practical applications in analytical mass spectrometry.

3.3 Laser-Based VUV Light Sources

Despite being considerably more complex than discharge and electron beam-pumped lamps, laser-based sources have several advantages because they produce pulsed and coherent radiation. Such light can be guided over longer distances by conventional optics, and it has a narrow bandwidth and high spectral purity. Many laser-based sources for VUV radiation rely on frequency tripling of intense laser pulses in low pressurized rare gas or rare gas mixture cells. A common setup for VUV light generation applying this principle uses the third harmonic wavelength (355 nm) of a Nd:YAG solid-state laser. Laser pulses of this frequency are focused in a stainless steel gas cell containing xenon with a pressure in the range between 10 and 50 mbar. If the local laser intensity at the focal point is sufficiently high, the electric field force becomes strong enough to produce a nonlinear dependency of the electron polarization. This leads to the generation of frequency-tripled radiation for about 0.001% of the 355 nm photons, yielding pulsed 118 nm radiation that leaves the cell through a MgF_2 window. The conversion depends heavily on a successful matching of the phase velocities of the fundamental and frequency-tripled wavelengths to avoid destructive interference of the two beams. This can be controlled by adjusting the pressure of the rare gas medium. Although the frequency tripling seems to be a very ineffective process at first glance, the resulting photon intensities are sufficient to utilize them in analytical SPI-MS applications. The conversion can be enhanced by replacing xenon with a mixture of argon and xenon (ratio approximately 10 : 1). Because of the different refractive indices of argon and xenon for 355 and 118 nm radiation, respectively, a better phase matching of the beams is possible, leading to constructive interference through adjustment of the phase velocities.

Pulsed fixed frequency VUV radiation can also be accessed directly by applying a fluorine excimer laser. The laser medium is a gaseous mixture of 1% F_2 in helium. Upon electrical excitation, F_2-excimers are formed, which by their decay yield laser pulses of 157 nm. The value for applications involving ionization for mass spectrometry is however limited to molecules exhibiting ionization energies below 7.8 eV. This restriction also holds for other VUV sources based on direct emission of laser radiation such as a novel laser-type operating with frequency doubling of the third harmonic of a Nd:YAG laser, resulting in laser pulses of 177.3 nm.

Figure 3.1 gives an overview of the emission spectra obtained from most of the described VUV light sources.

Four-wave sum mixing provides the possibility to extend the wavelength region of laser-based VUV radiation down to the threshold of the LiF window (105 nm). The VUV generation however requires a sophisticated setup with two dye lasers,

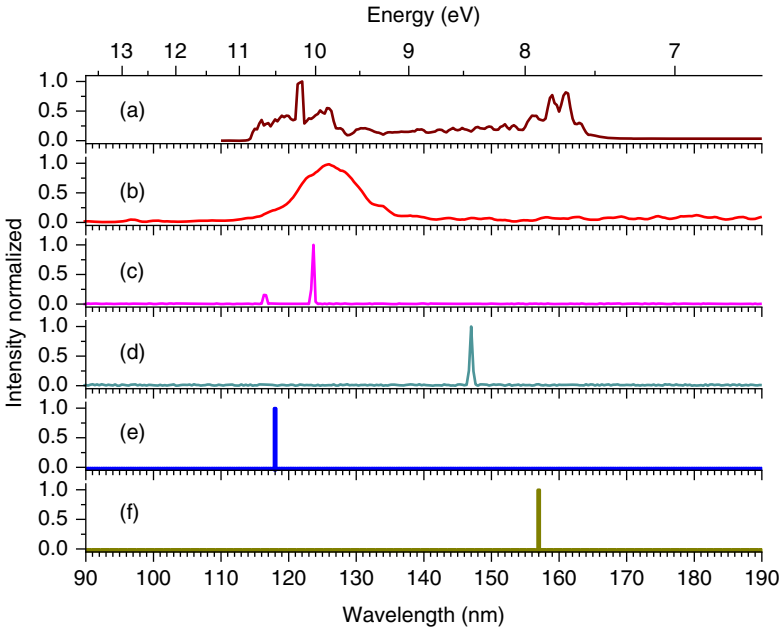

Figure 3.1 Measured emission spectra of different VUV light sources in the wavelength range between 90 and 190 nm, corresponding to photon energies from 6.5 to 13.75 eV (VUV spectrometer with low resolution monochromator): (a) D_2-Lamp (McPherson), (b) Ar-Electron beam-pumped lamp, (c) Kr-discharge lamp (PID), (d) Xe-discharge lamp (PID), (e) ninth harmonic frequency of the Nd:YAG laser line (sketched), and (f) F_2-Excimer laser line (sketched).

each pumped by a Nd:YAG laser. The output of one dye laser in the visible region is frequency doubled and the resulting UV light is tuned to excite a two-photon resonance transition in xenon gas. The second dye laser can be tuned in the visible region and focused to the same point in the xenon gas cell as the UV light. Sum mixing of the beams yields VUV radiation between 105 and 110 nm as output (Al-Basheer et al. 2011). The available span of VUV wavelengths is limited by the utilized dye for the visible region, and extending it to other VUV regions requires constant changing of the dye. Spectral purity constitutes a problem, however, because the initial UV and visible wavelengths are considerably more intense than the resulting VUV light and have to be separated from the VUV output. Replacement of dye lasers by optical parametric oscillators (OPOs) could overcome the limitation of frequent changing of the dye in the dye laser.

An elaborate setup in this context is four-wave difference mixing in xenon gas with one dye laser and one OPO (Hanna et al. 2009). The dye laser is used at a fixed frequency to excite a two-photon resonance of xenon and the OPO provides the tunable wavelength. This allows wavelength scanning between 122 and 168 nm (7.4–10.2 eV), while changing the dye only once. Both lasers produce narrow bandwidth light, which allows for high-resolution VUV scanning. A monochromator based on a single MgF_2 lens is incorporated to separate the generated VUV light from the pump wavelengths, thus ensuring high spectral purity. Careful computer control of the pump optics and the monochromator

lens yields a precisely positioned and uniformly sized beam even when scanning the VUV output.

Another variation of a laser-based VUV light source is the use of a plasma. This is produced by focusing the fundamental of an Nd-YAG laser (1064 nm) on a supersonic xenon gas jet (Di Palma et al. 2009). The resulting emitted radiation found to be continuous in the wavelength range between 100 and 200 nm, is collected, and spectrally dispersed by a concave flat-field diffraction grating.

A variety of new methods for generating VUV from ns, ps, and fs-pulsed lasers has been recently reviewed (Ubachs et al. 2014). The use of fs-pulse lasers for generation of VUV has also advanced, via both third harmonic and four-wave mixing in laser-generated plasmas in noble gas known as filaments (Horio et al. 2014; Wang et al. 2014). Finally, high harmonic generation (Chen et al. 2009; Popmintchev et al. 2015) of VUV in noble gas plasmas has been demonstrated but requires separation of VUV from extreme UV and higher energy harmonics. Most of the above methods have not been applied to photoionization mass spectrometry (PIMS). However, one example using high harmonic generation of VUV for PIMS was in photoion–photoelectron coincidence spectroscopy of pyrolysis products (Couch et al. 2017).

3.4 Mass Spectrometry with Lamp or Laser-Based VUV Light Sources

The application of VUV radiation for vacuum ionization in mass spectrometry, which proceeds by absorption of a single photon (thus single-photon ionization, SPI, see Chapter 1), is attainable in several variations. The first general distinction comes with the manner of VUV radiation utilized for ionization, i.e. if VUV light is emitted pulsed or continuous. Either way affords an appropriately adapted ion source. Secondly, the mass spectrometric unit may differ. Quadrupole instruments work conveniently with continuous VUV light sources, while time-of-flight (ToF) devices require special layout depending on the nature of the VUV light. Even ToF systems with quadrupole ion traps have been reported as detection units for VUV light-generated ions, which is elaborately described later in this section.

Staying with time-of-flight mass spectrometers, there are two general setups in use. Principle sketches of such setups are depicted in Figure 3.2. The left sketch (Figure 3.2a) shows the combination of a continuously working VUV lamp with a time-of-flight mass spectrometer (ToFMS) employing an orthogonal extraction of the ions (orthogonal acceleration time-of-flight massspectrometer, oaToFMS). Herein, the ions are accelerated perpendicularly to their initial direction of motion, shown by the red curve visualizing the flight path. Pulsed laser VUV light sources work best with a direct reflectron ToFMS that accelerates the ions generated from each VUV laser light pulse in the ion source directly as a package into the flight tube (Figure 3.2b). Unlike ToFMS systems, Ion Trap Mass Spectrometry (ITMS) allows easy access to tandem mass spectrometry (MS/MS, Schramm et al. 2009a, Schramm et al. 2009b). Here in particular the combination of soft ionization by SPI (i.e. for efficient and low interference

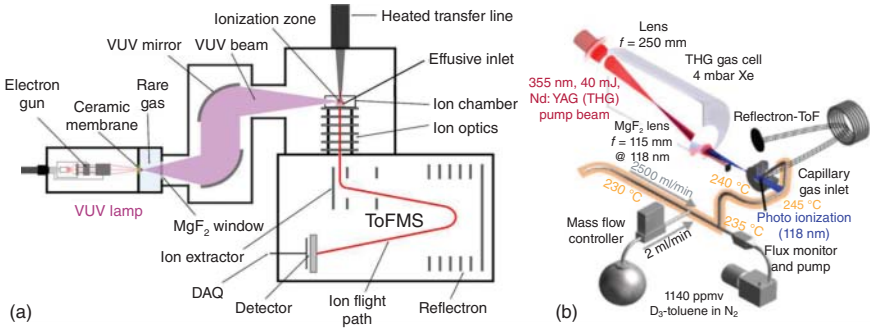

Figure 3.2 (a) Setup of a VUV lamp-based SPI-ToF mass spectrometer. In the depicted scheme, an electron beam-pumped excimer lamp (EBEL) using argon as active species is applied as the VUV beam source (the spectrum of Ar EBEL lamp depicted in Figure 3.1). Analyte mixtures are introduced to the ion source via a heated capillary transfer line. After ionization, a continuous primary ion beam is formed. In an ion extractor unit, ion packages are orthogonally accelerated into the ToFMS flight tube by means of pulsed high voltages (orthogonal acceleration ToFMS). (b) Setup of a laser-based SPI-ToF mass spectrometer. In the depicted scheme, a ninetupled, pulsed Nd:YAG laser is applied as a VUV laser beam source. The resulting 118 nm emission line of a frequency-tripled Nd:YAG third harmonic wavelength of 355 nm is depicted in Figure 3.1 as well. The analyte mixtures are introduced to the ion source via a heated capillary transfer line. Deuterated toluene is added as an internal standard. The generated ion packages are directly extracted into the flight tube of the reflectron ToF. Source: Modified after Czech et al. (2016a).

formation of molecular ions) and collision induced dissociation/fragmentation (CIA) of selected precursor ions in MS/MS is beneficial.

3.5 On-line Analysis of Complex Mixtures by Single-Photon Ionization (SPI) Mass Spectrometry

The unique feature of using VUV radiation for ionization of molecules in the vacuum is the very soft ionization characteristics of the resulting single-photon ionization process. The fact of generating almost fragment-free molecular ions makes SPI a natural choice for the characterization of complex mixtures, where hard ionization methods such as electron ionization (EI) reach their limits because of heavy overlapping of fragment ions, small or negligible intensity of molecular ions, and the difficulty of discerning species that produce the same fragments. Moreover, these unfragmented molecular ions may be used for quantitative analysis. Despite the soft character of SPI, there are some substance classes that could not be ionized without fragmentation. Among these are some alcohols that show a dominant fragment ion because of the loss of neutral water, and highly branched alkanes that tend to form stabilized secondary and tertiary carbenium fragment ions. These fragmentation pathways require very little or sometimes no excess energy above the ionization threshold and therefore come to pass even with ionization by VUV light.

When SPI with VUV photons is combined with a fast mass spectrometric detection method such as ToFMS, its soft nature makes it easily eligible for

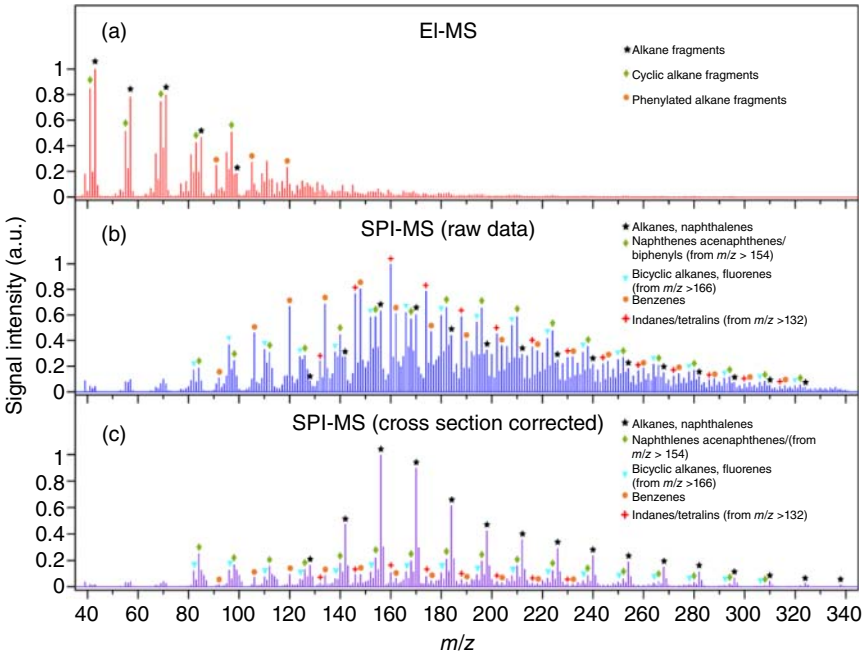

Figure 3.3 Three mass spectra of a mineral oil-type fuel (diesel fuel, fully vaporized). (a) 70 eV EI mass spectrum obtained by summing up over the total gas chromatographic run. (b) SPI mass spectrum (raw data) obtained by summing up over the total gas chromatographic run. (c) Cross section corrected SPI mass spectrum (averaged cross sections for compound classes) approximating the molar concentration profile of the mineral oil distillate sample. Source: Modified from Eschner et al. (2011b).

on-line monitoring of dynamic processes. A further advantage lies in the upper threshold of photon energies accessible with SPI because it precludes ionization of most background and bulk gases such as nitrogen, oxygen, water, and carbon dioxide because of their higher ionization energies. Therefore, ions of such bulk species do not interfere with SPI-ToFMS signals of the organic trace analytes (i.e. by detector saturation or scattered ion background).

Figure 3.3 depicts a comparison of a complex mixture mass spectrum analyzed by electron ionization – time-of-flight mass spectrometry (EI-ToFMS) and single-photon ionization-time-of-flight mass spectrometry (SPI-ToFMS), vividly demonstrating the benefit of soft ionization for the characterization of complex samples (diesel fuel in this case). The figure also reveals the effect of varying ionization efficiency for different substance classes, whereby unsaturated species generally show larger response to SPI.

Among the most widespread real-world applications with a highly dynamic behavior are combustion and pyrolysis processes. Hence, it is obvious that a relatively large number of single-photon ionization-mass spectrometry (SPI-MS) applications occupy themselves with the on-line monitoring of emitted off-gases from such processes. In Figure 3.4, SPI mass spectra of different on-line measurement applications are depicted: exhaled breath of a smoker before (a) and after consuming a cigarette puff (b), gasoline car exhaust gas (c), tobacco smoke

(d), coffee-roasting process gas (e), and finally process gases of an industrial biomass pyrolysis pilot plant (f). The figure demonstrates the "fingerprinting" capability of soft photoionization mass spectrometry. In the mass spectrum of the exhaled breath before smoking shown in Figure 3.4a, two of the main organic compounds of the human metabolism of healthy subjects are visible: acetone (m/z 58) and isoprene (m/z 68). In contrast, the mass spectrum of exhaled breath of a smoker shortly after smoking depicted in Figure 3.4b shows a large number of xenobiotic compounds including the homologous series of alkenes (◆), dienes (●), carbonyl compounds (aldehydes and ketones, ○), alkylated benzenes (▲), and alkylated phenols (■), which also occur in tobacco smoke itself. Figure 3.4c exhibits an on-line measured mass spectrum of gasoline car exhaust, which is dominated by unburnt fuel components such as alkylated benzenes (▲), alkanes (▼), and alkylated naphthalenes (□) as well as combustion products such as alkenes (◆), dienes (●), and alkylated styrenes (★). Partially, these

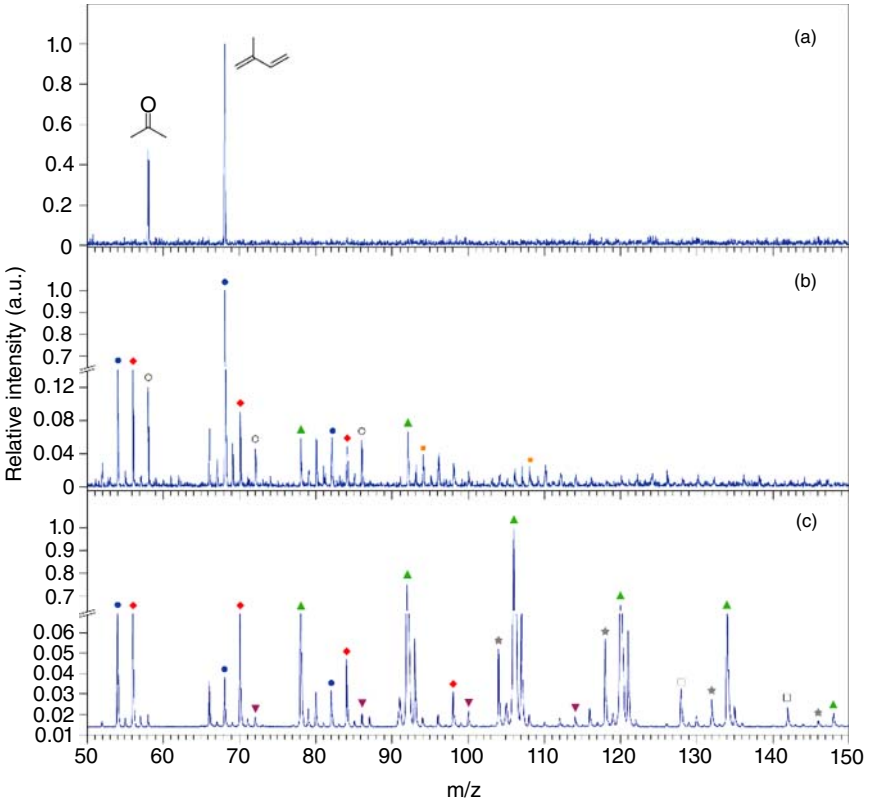

Figure 3.4 SPI mass spectra from different on-line measurement applications (normalized according to the highest peak): (a) exhaled breath of a smoker before smoking, (b) after consuming a cigarette puff, (c) gasoline car exhaust gas, (d) tobacco smoke, (e) coffee-roasting process gas, and (f) process gases of an industrial biomass pyrolysis pilot plant. The measurements were performed with an EBEL VUV lamp time-of-flight mass spectrometer (panels a, b, c, d, and f) or an EBEL VUV lamp ion-trap mass spectrometer (panel e). Source: unpublished data from authors

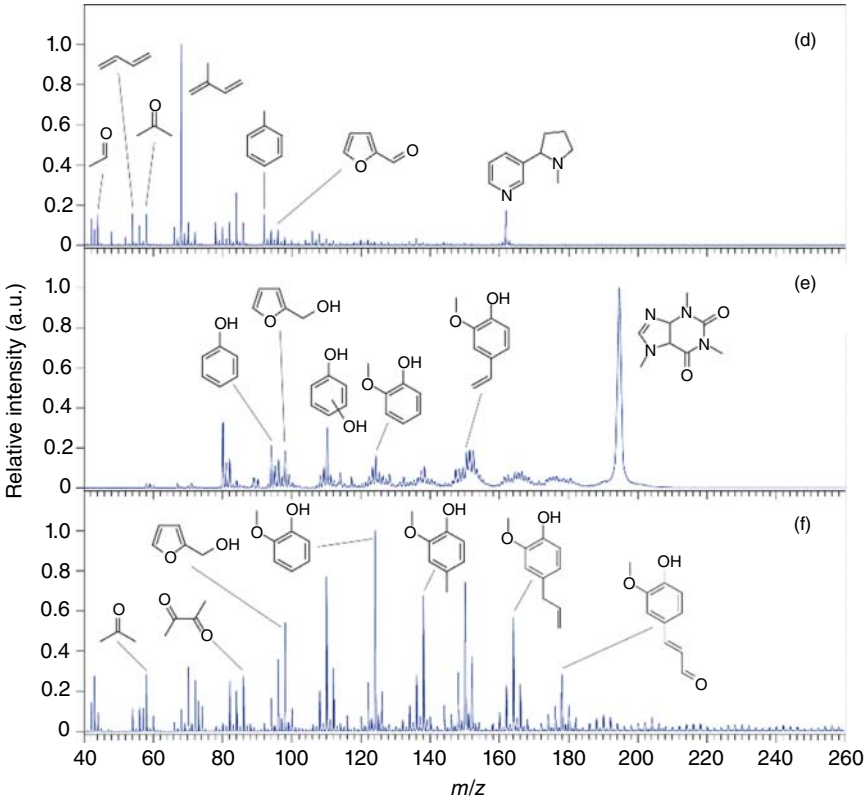

Figure 3.4 (*Continued*)

compounds show isobaric interferences. The mass spectrum of tobacco smoke depicted in Figure 3.4d exhibits combustion products such as 1,3-butadiene (m/z 54) and isoprene (m/z 68) as well as plant material pyrolysis species such as acetaldehyde (m/z 44) and furfural (m/z 96) and, of course, the main alkaloid in tobacco leaves, nicotine (m/z 162). Note that tobacco smoke also contains the homologous series already assigned in exhaled breath (see Figure 3.4b). The SPI mass spectrum of coffee-roasting gas using an ion-trap mass spectrometer is depicted in Figure 3.4e. The most prominent peak caffeine (m/z 194) and some phenolic compounds such as phenol itself (m/z 94), dihydroxybenzenes (m/z 110), guaiacol (m/z 124), and 4-vinylguaiacol (m/z 150) as well as furfuryl alcohol (m/z 98) are assigned. Figure 3.4f shows an SPI mass spectrum recorded at an industrial pilot plant for biomass pyrolysis. The mass spectrum comprises phenolic compounds (m/z 110, 124, 138, 150, 164, and 178) yielded by degradation of lignin and carboxylic (m/z 44, 58, and 86) as well as furan derivatives (m/z 96 and 98) yielded by pyrolysis of cellulose. Note that in cases where more than one isobaric compound is populating peaks, the predominantly occurring compound is assigned.

In Figure 3.5, profiles of selected molecular mass traces over time taken from the on-line process measurements associated with the on-line measured SPI

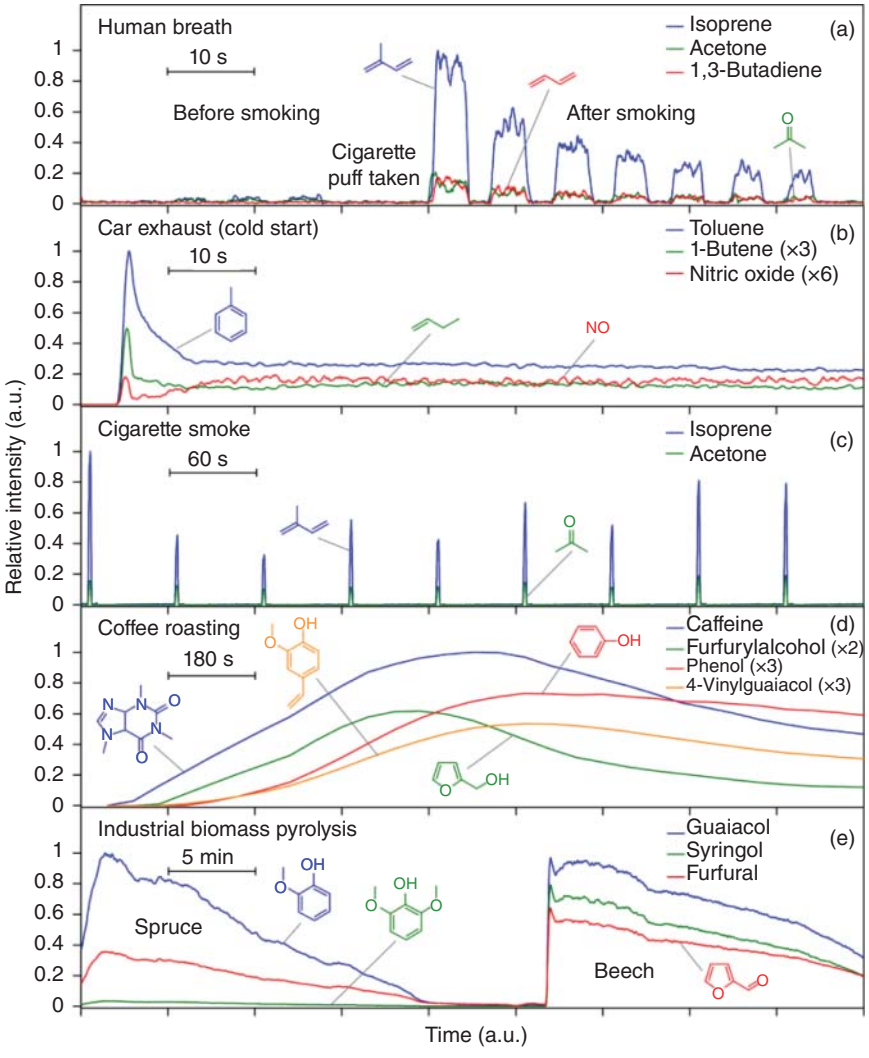

Figure 3.5 Time profiles of selected masses from on-line SPI-MS measurements using a VUV lamp for ionization (Ar-EBEL, see Figure 3.4 for SPI mass spectra): (a) human breath analysis, (b) monitoring of car exhaust gases, (c) analyzing cigarette smoke, (d) monitoring of coffee-roasting process, and (e) analyzing pyrolysis gases from an industrial biomass plant. The measurements were performed with an EBEL VUV lamp time-of-flight mass spectrometer (panel a, b, c, and d) or an EBEL VUV lamp ion-trap mass spectrometer (panel d). Source: unpublished data from authors.

mass spectra of Figure 3.4 are depicted. The benefit of real-time on-line measurements is obvious when transient processes are studied. For better visualization, the timescale of each measurement is divided into nine parts, whereas in each panel, the horizontal bar indicates the time of one subunit, respectively. In Figure 3.5a, the inhale–exhale profile of isoprene and acetone of a smoker before and after the first puff on a cigarette is depicted. During the measurement, the subject was breathing through a tube from which a small sample stream was taken

continuously. Thus, alternately exhaled breath and fresh inhaled air were sampled with the frequency of the breath cycle. The first three breath cycles in Figure 3.5a show the concentration profiles of isoprene, acetone, and 1,3-butadiene before smoking. Then, the subject is taking a cigarette puff as indicated. The first exhalation exhibits an increased amount of these three compounds because of their high content in cigarette smoke (see Figure 3.4d). In the following, the concentration of these compounds declines from breath cycle to breath cycle, showing the clearance of the lungs. In Figure 3.5b, the concentration of selected compounds in the exhaust of a gasoline-fuelled car equipped with a catalytic converter during a cold start is depicted. At engine start, high concentrations of unburnt fuel (toluene, m/z 92) and combustion products such as 1-butene (m/z 56) and NO (m/z 30) occur. With proceeding time of idling, the catalytic converter is heating up, getting slowly more and more effective. This is reflected in the decay of toxic air pollutants in the exhaust. In Figure 3.5c, the time profiles of 1,3-butadiene (m/z 54) and nicotine (m/z 162) from cigarette smoking are depicted. The puff structure of two seconds is clearly visible, demonstrating the high time resolution. Figure 3.5d shows the profile of some volatiles in coffee-roasting gas. At about 12 minutes, caffeine (m/z 194) and furfuryl alcohol (m/z 98) reach their maximum while phenol (m/z 94) and 4-vinylguaiacol (m/z 150) still increase. The detected different time profiles of these components allow the application of SPI-MS for on-line controlling of the coffee-roasting process. Figure 3.5e depicts the time profiles of the selected phenolic species guaiacol (m/z 124) and syringol (m/z 154) as well as the furan derivative furfural (m/z 96) in the pyrolysis gas of a biomass reactor plant (KIT, Karlsruhe, Germany). During a measurement campaign, changes of feedstock and other process parameters were investigated. In the part of the experiment shown, the feed was changed from spruce (softwood) to beech (hardwood) detected by a decline of all masses. For softwood, the ratio of syringol to guaiacol is about 0.07, while it is about 0.7 for hardwood. Both feeds are interesting for the biomass-to-liquid (BTL) process (KIT, Karlsruhe, Germany) for generation of liquid diesel-like fuel from renewable carbon dioxide-neutral feeds, where flash pyrolysis represents the first step of this process.

The examples discussed above show the strength of the SPI-MS approach for on-line analysis of even highly complex substance mixtures. In the following, some on-line measurement applications applying the SPI-MS approach are presented in more detail. In this regard, the study of exhaust gases from internal combustion engines constitutes an application of common interest (Yamamoto et al. 2012). SPI-ToFMS can register dynamic concentration changes of hazardous organic trace compounds such as butadiene, 2-propenal (acrolein), or benzene caused by variations in load or acceleration events as well as changes in the performance of exhaust gas treatment catalysts (Adam and Zimmermann 2007). Time-resolved chemical profiles of organic species present in the emitted exhaust gases of several other combustion and pyrolysis processes have also been investigated. Waste incineration (Kuribayashi et al. 2005; Liu et al. 2016), biomass combustion (Czech et al. 2016a) and pyrolysis (Fendt et al. 2012; Jia et al. 2015), coal pyrolysis (Xu et al. 2017), thermal decomposition of polymers (Wang et al. 2015), and coffee roasting (Dorfner et al. 2004) are representative examples. In all such applications, it becomes possible to monitor a broad range of organic trace compounds containing a large variety of functional groups in low-concentration

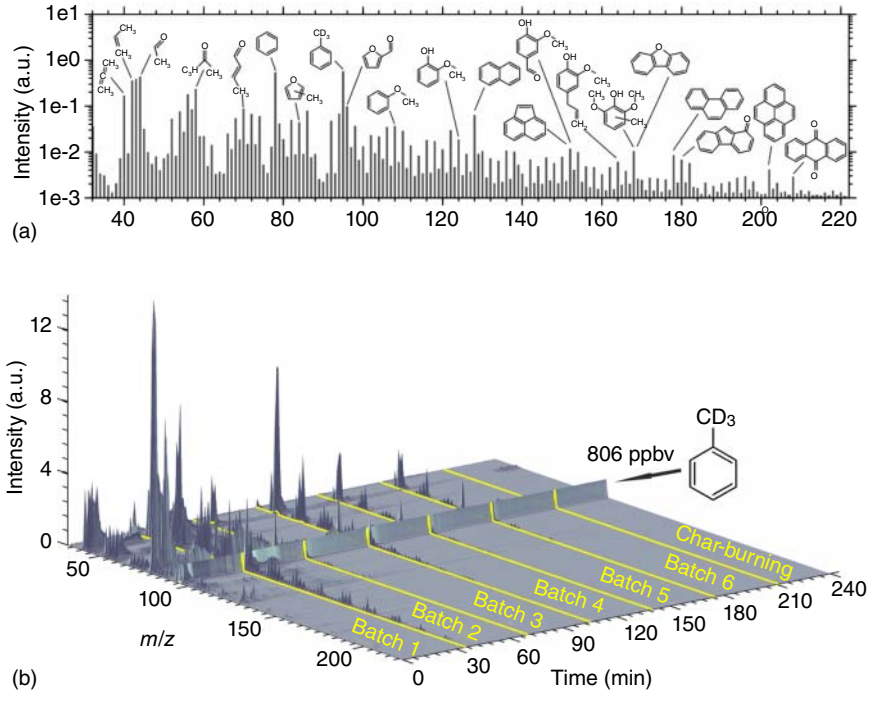

Figure 3.6 (a) Time-resolved SPI mass spectra, normalized to the peak intensity of the deuterated toluene at *m/z* 95, of a combustion experiment with beech logwood, depicting six consecutive batches of wood loading. (b) Averaged mass spectrum of the whole combustion experiment showing the versatile detection availability for different kinds of substance classes present in the exhaust gas of wood combustion. Source: Czech et al. (2016a).

ranges (parts-per-billion to parts-per-million range). The monitoring thereby proceeds in real time with a high time resolution independent of the nature of the complex gaseous matrix. The special attribute of SPI is the ability to study aliphatic compounds with or without heteroatoms (alkanes). Note, that soft ionization of alkanes is difficult for many other ionization techniques in mass spectrometry, such as electron ionization (EI, too much fragmentation), chemical ionization (CI, no ionization), electrospray ionization (ESI, no ionization) or atmospheric pressure chemical ionization (C, no ionization).

The following three examples serve to illustrate more precisely the usefulness of SPI-ToFMS for the characterization of organic trace compounds formed in combustion or pyrolysis processes. Figure 3.6b shows the four-hour monitoring of beech wood combustion in a masonry heater. The dynamics of the process is highlighted quite effectively here. In the beginning, at cold conditions, considerably high emissions of aromatic and phenolic species are observed, and at the beginning of every new batch, the emissions sharply increase as well. However, with proceeding time, the effects gradually diminish when the stove gets warmer; thus, with every new batch, the increase of organic emissions becomes less pronounced and concentrations fall down rather quickly, reaching the limits of detection for many species. The graph (Figure 3.6a) shows the corresponding mass spectrum averaged over the whole four-hour experiment. A rather rich

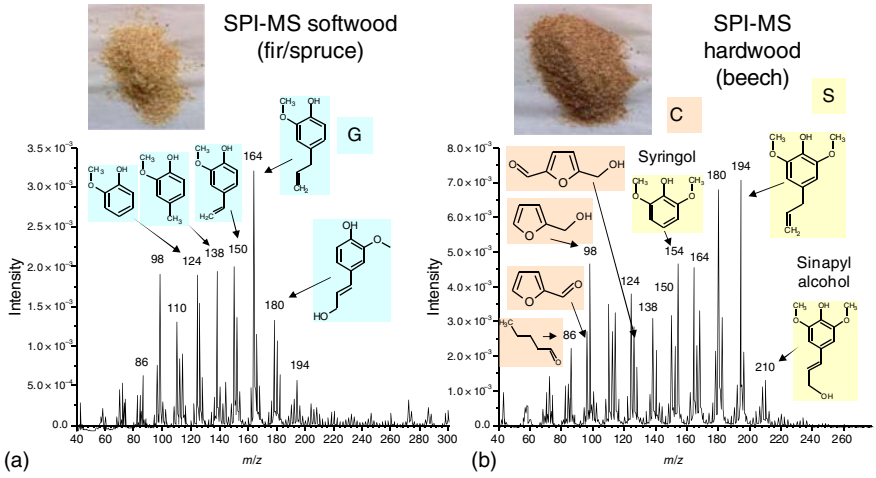

Figure 3.7 Emerging gas-phase products from wood pyrolysis recorded by real-time SPI-ToFMS depicting differences between softwood (a) and hardwood (b) via the respective patterns of phenolic and furanoic species. G stands for guaiacol derivatives, S for syringol derivatives, and C for cellulose decomposition products. See also: Fendt et al. (2012).

conglomeration of organic substances is accessible with SPI-ToFMS, ranging from small alkenes as typical pyrolysis products of larger hydrocarbon structures to three- and four-ring polycyclic aromatic hydrocarbons as likewise typical products of incomplete combustion of carbonaceous fuels. In the middle section of the accessible mass range, phenolic and furanoic compounds are detected, which are produced by thermal decomposition of the main constituents of wood cellulose and lignin, respectively.

Figure 3.7 shows SPI mass spectra of the primary pyrolysis products of two feedstocks during flash pyrolysis experiments. The spectra were on-line recorded (process gas) at a biomass flash pyrolysis pilot plant reactor. The flash pyrolysis step represents a sub-process in the scheme to produce organic chemicals or fuel from biomass. With SPI-ToFMS, the differences between variable feedstocks are easily carved out, and the changing pattern of phenolic species and products from cellulose decomposition proves to be unique for each feedstock material. Softwood pyrolysis yields predominately phenolic compounds formed by thermal degradation of guaiacyl-like lignin units (referred to as G-units in blue). Contrary, pyrolysis of hardwood shows syringyl-like fractions of phenolic species (referred to as S-units in yellow), reflecting the different kinds of lignin that dominate in the structural composition of each wood type. In addition to that, both wood types also yield decomposition products from cellulose (referred to as C-units in ocher), which are mostly furanoic compounds such as furfural (96 m/z) or furfuryl alcohol (98 m/z). The recording of such mass spectra displaying the primary pyrolysis products from different types of biomass offers an insight into the composition of the applied feedstock material.

The final example deals with a unique approach for getting closer to the understanding of the coffee-roasting process. Photoionization ToFMS is able to monitor the roasting process of coffee bean batches (see also Chapter 3 for resonance-enhanced multiphoton ionization mass spectrometry applications

for coffee-roasting process monitoring). The process can also be scaled down to the investigation of a single bean. For this, SPI-ToFMS is carried out with a microprobe as the sampling device, which is inserted inside a coffee bean (Figure 3.8c). The microprobe samples off-gases directly from inside the bean, when it is heated with a temperature program simulating the coffee-roasting process (Hertz-Schünemann et al. 2013). By doing this, alkenes, carbonyls, furans, and phenol derivatives as well as caffeine and fatty acid are detected, as is shown in the corresponding mass spectrum to the right (Figure 3.8d). Subtle differences in the spectra between Arabic and Robusta coffee beans are revealed, which may serve as an easy method for distinguishing these varieties, as shown in Figure 3.8a for cafestol and kahweol.

In a roasting experiment with a small-scale drum roaster having a batch size of 100 g, the microprobe sampling approach in connection with SPI-ToFMS enables the visualization of coffee-roasting phases (Czech et al. 2016b). Non-negative matrix factorization (NMF) decomposes the non-negative m/z-by-time matrix of on-line mass spectra into a k-by-time score matrix and a m/z-by-k loading matrix. The dimension k denotes the number of factors and may be regarded as the number of subprocesses contributing to the mass spectra matrix. Because of the restriction to the non-negative range of numbers, the factor loadings can be interpreted as a representative "feature mass spectrum", which is depicting the mass spectrometric signals of the chemicals relevant for those subprocesses, i.e. the coffee-roasting phases "evaporation," "early roast," "late roast," and "over-roast." The score matrix contains the contribution of each roasting phase for every point of time, allowing, for example, the increased formation of over-roast indicators such as pyridine (m/z 79).

For process control, it is essential to obtain information about the status of roasting in real time, e.g. roast degree measurement by color value (Colorette System, Probat, Germany), such as antioxidant capacity of the coffee brew measured by antioxidant assays. Both types of measurements are done off-line, are time-consuming, and labor-intensive. However, if this was done for a sufficient number of roast events, those coffee properties can be linked to the mass spectra from the analysis of the roasting gas at coffee bean drop temperature by partial least square (PLS) regression. In a exemplary study, the roasting gas from different roasts of Columbian Arabica coffee was analyzed by laser-based SPI-ToFMS at 118 nm in order to generate explanatory PLS regression models for roast degree and antioxidant capacity, determined by color value measurement (Colorette, dimensionless value) and Folin–Ciocalteu (FC) assay (in equivalent mass of gallic acid per liter [GA-eq. mg/L]). The root-mean-square error of the cross-validation ($RMSE_{CV}$) accounted for ±6.0 in color value and ±139 GA-eq. mg/L, which is equal to relative precisions of 6.8% and 4.4% related to the mean of color value- and FC value-range (Heide et al. 2020). From the target projection (tp) loadings, the variable importance for the calculation of the coffee property can be assessed. The softness as well as the sensor-like selectivity of the ionization simplifies the interpretation of the tp loadings. Hydroxymethylfurfural (m/z 126) and 2,3-dihydro-3,5-dihydroxy-6-methyl-4*H*-pyran-4-one (m/z 144) were the most important variables to explain the variance between SPI mass spectra, roast degree (color values) and antioxidant capacity (FC values), respectively. Finally, the explanatory model was applied to on-line recorded SPI mass spectra

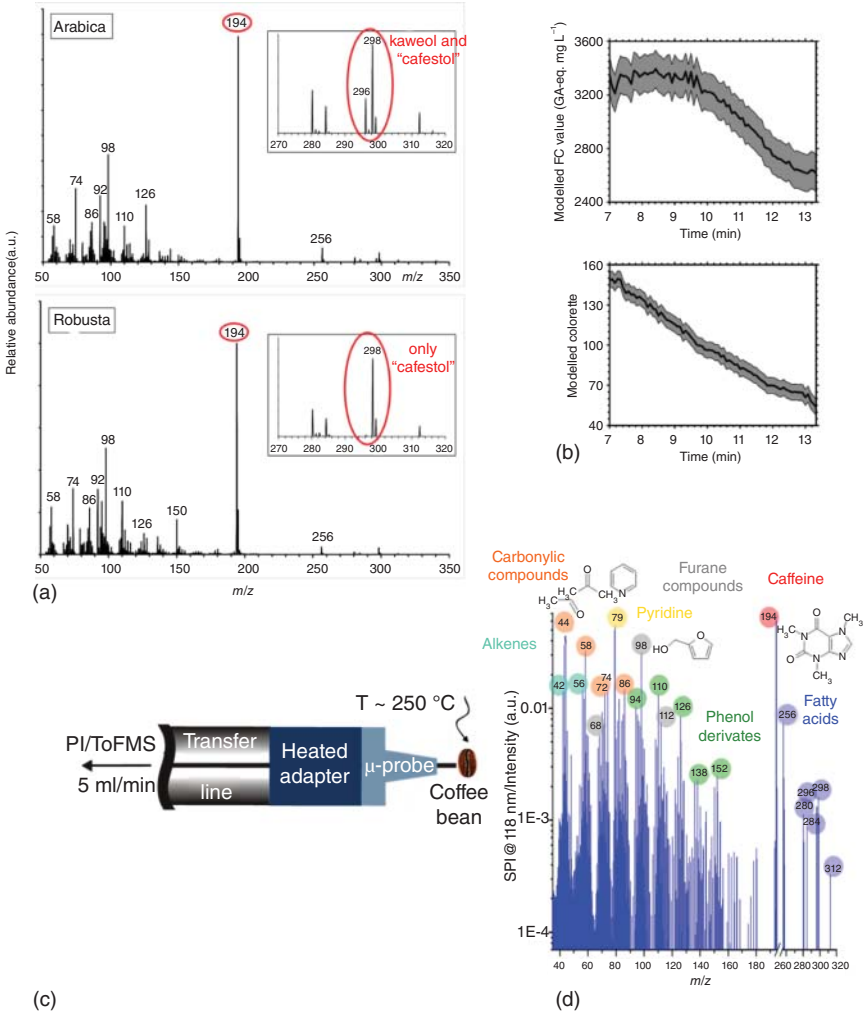

Figure 3.8 SPI mass spectrometry results (PhotoTOF-process monitor, Photnion GmbH, see section 3.8) (a) SPI-ToFMS mass spectra from the roasting gas of the coffee species Arabica and Robusta show a characteristic difference in the occurrence of lipids. (b) Application of explanatory model for roast degree and antioxidant capacity (based on color value and Folin-Ciocalteu assay) via SPI-MS monitoring of an individual roast, demonstrating that the photoionization mass spectral fingerprint can be used for coffee roasting process control. (c) Setup for microprobe sampling of gaseous compounds from inside a coffee bean. (d) SPI-ToFMS spectrum obtained after microprobe sampling from a roasted coffee bean.

of an individual roast to illustrate the potential of this technique for process control (Figure 3.8b, Heide et al. 2020) and motivates a follow-up study (Czech et al. 2020), deploying REMPI-ToFMS spectra for PLS regression models as well.

The investigation of organic substances in cigarette smoke is a further special application of SPI-ToFMS because it allows following concentration trends of toxic components in every consecutive puff taken (Adam et al. 2006; Mitschke

et al. 2006a). If smoking is carried out with a smoking machine device complying with standard protocols, every puff lasts two seconds. However, even during this small time span, concentrations of some substances can vary by several orders of magnitude. Figure 3.9a shows a three-dimensional depiction of the complete smoking process of a cigarette (mainstream smoke, i.e. the smoke which is inhaled) recorded by direct inlet SPI time-of-flight mass spectrometry via a smoking machine. Concentration variations of the puff by puff emitted gaseous chemicals become visible. The emission profile of chemicals in the sidestream smoke (i.e. the smoke that is is emitted from the cigarette to the environment) during the smoking process is depicted in Figure 3.9b. Due to the smoldering between the puffs here the release profile with time appears blurred. In addition to nicotine, a variety of toxic gaseous tobacco smoke constituents (acetaldehyde, 1,3-butadiene, acetone, isoprene, toluene, among many others) are observed in the SPI mass spectra of main- and sidestream smoke. Different temporal progression of individual compounds can be observed. This is shown exemplary for a mainstream smoke measurement (Figure 3.9c) depicting 1,3-butadiene and nicotine. While the concentration of the highly toxic and carcinogenic butadiene in the first puff is considerably high, followed by a steep drop in the second puff, nicotine shows a steady and gradual puff-per-puff increase. This so-called "first puff high" effect occurs for several unsaturated molecules, which are considered as primary combustion intermediates. The reason for this effect is the nonoptimal combustion condition of the partly cold cigarette tip during the lighting process. The gradual increase of nicotine (and 1,3-butadiene starting from the second puff) is due to the decrease of the cigarette length and the accompanied reduction of dilution air by cigarette paper diffusion as well as due to absorption at the still cold tobacco rod and the later redesorption by the propagating glowing front.

Microprobe sampling offers additional insights into the processes occurring inside a cigarette rod by analyzing the spatial distribution of compounds directly at the location of their formation (Hertz-Schünemann et al. 2015). Figure 3.10a,b shows a scheme and a photograph of the microprobe, respectively, where it is inserted inside the cigarette rod during a smoking experiment. Repeating the smoking process under standardized conditions and varying locations for the insertion of the microprobe's tip renders it possible to visualize a two-dimensional distribution of selected compounds during the smoking of a cigarette. This is depicted in Figure 3.10c for nitrogen monoxide and benzene measured with SPI-ToFMS, demonstrating high NO concentrations at the tip of the burning zone and high benzene concentrations in the pyrolysis zone of the cigarette.

SPI-MS is a feasible method for human breath gas analysis (Kleeblatt et al. 2015; Wang et al. 2016). The breath gas of animals such as mice can also be investigated by SPI-MS in order to reveal metabolic processes (Zhang et al. 2017). It is remarkable in this respect that elevating the pressure in the ion source could help to improve the limits of detection down to the ppt range. (Wang et al. 2016). In the latter case, however, matrix effects due to chemical reaction/ionization effects cannot be any longer excluded.

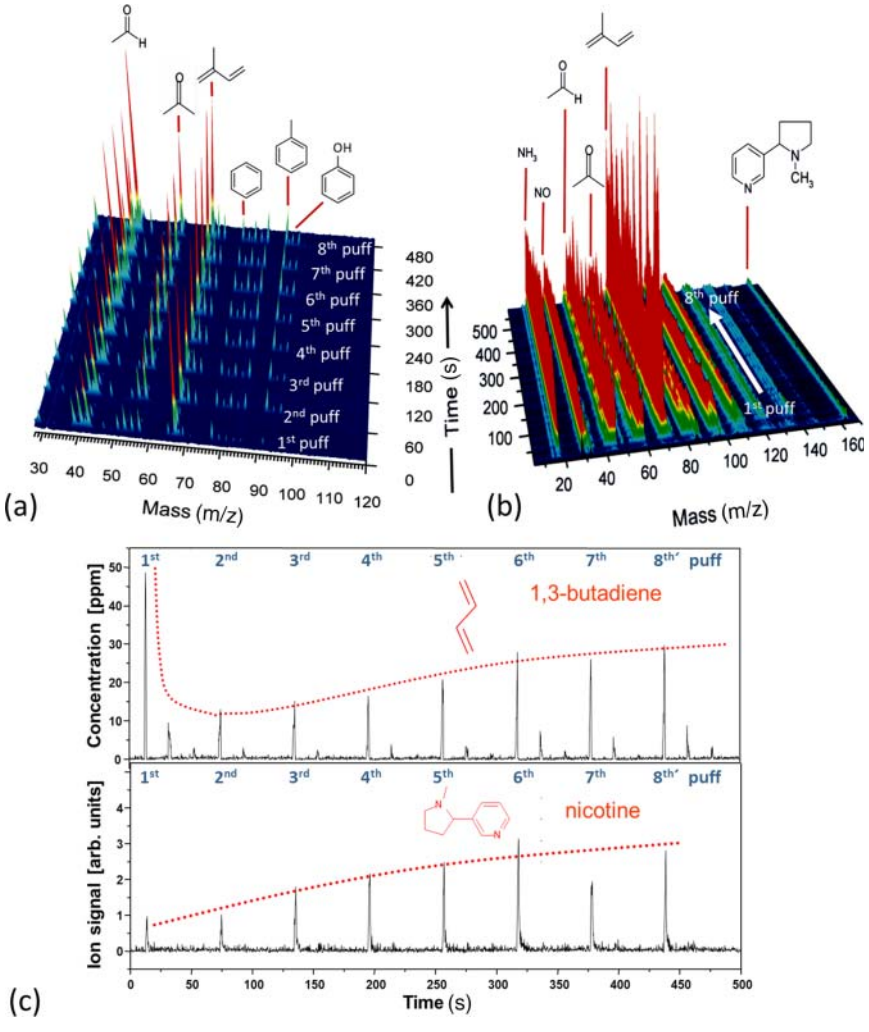

Figure 3.9 Puff-to-puff resolved SPI-ToFMS measurement of cigarette smoke generated by a smoking machine (ISO-smoking profile, one bell-shaped 35 ml 2-second lasting puff per minute). (a) 3D representation of a time-resolved SPI-ToFMS mainstream smoke measurement. The sharply resolved individual puffs are indicated. (b) 3D representation of a time-resolved SPI-ToFMS sidestream smoke measurement. Due to the smoldering emission between the puffs, the puff structure appears blurred. (c) Temporal concentration trends of two selected compounds, 1,3-butadiene and nicotine (ISO-profile), extracted from data shown in (a) (peaks between puffs are due to sampling line cleaning procedure). The high concentration of 1,3-butadiene in first puff is due to the non-optimal combustion conditions during the ignition phase and the increasing concentration of nicotine with puff-number is due to nicotine adsorption/re-desorption effects in the tobacco rod driven by the propagating amber front and the reduction of through-paper dilution air with the reducing length of the cigarette. Source: Modified from Mitschke et al. (2006a).

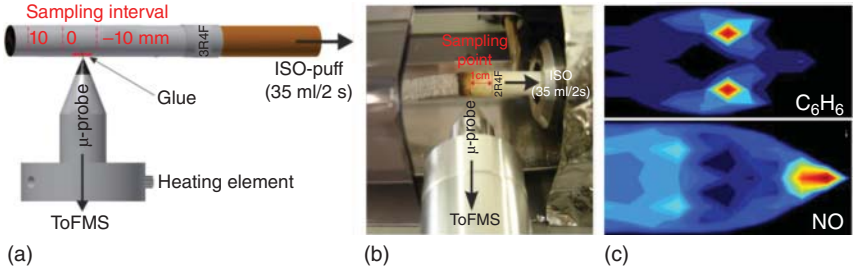

Figure 3.10 (a) The scheme of the cigarette mapping experiment – sampling approach shows the grid pattern of the sampling locations. (b) Photograph of the microprobe inserted into the cigarette rod during a standardized machine smoking experiment (ISO conditions). (c) Exemplary result: the two-dimensional heat map distributions of NO and benzene (black – lowest to red – highest concentration) immediately after the beginning of a puff clearly depict the different formation and destruction zones in the tip of the cigarette. Source: Zimmermann et al. (2015). Reproduced with permission of American Chemical Society.

SPI-MS also has the potential for forensic and security relevant applications. This includes the sensitive and selective detection of explosives, chemical warfare agents, illegal drugs, and their precursors see e.g. (Mullen et al. 2006). Figure 3.11 shows an example for such an application of mobile, van based SPI-MS unit for the detection of 3,4-methylenedioxymethamphetamine (MDMA) (ecstasy). A wipe pad is used to get a sample from a place where the drug is suspected. After thermal desorption, the evaporated constituents of the sample are guided into the ion source of an ion trap mass spectrometer, where they are ionized by VUV light of a lamp. MDMA is identified by its molecular ion in a MS/MS experiment on the basis of its fragment ions (Schramm et al. 2009a, Schramm et al. 2009b).

Applications of SPI-MS are not restricted to the detection of organic molecular species but could act as a method for the fundamental investigation of the gas-phase chemistry of neutral metal oxide or sulfide clusters (Yin and Bernstein 2012) and rare gas clusters (Bauer 2004).

3.6 SPI-MS in Hyphenated Applications

Mass spectrometry is a universally applied detector for various separation techniques such as gas chromatography (GC), comprehensive two-dimensional gas chromatography (GC × GC), and liquid chromatography (LC). Furthermore, it can be applied as a means of evolved gas analysis (EGA) to characterize the effluents of thermal analysis methods such as thermogravimetry. In many cases, electron ionization is utilized for these tasks, and there are numerous devices commercially available worldwide. However, application of SPI in such detector systems can provide unique insights not accessible with EI.

When SPI-MS is coupled to gas chromatography, it is adding additional capabilities to the analytical power of the hyphenated instrument that transcend the mere functionality as a detector for the separated compounds. Because the

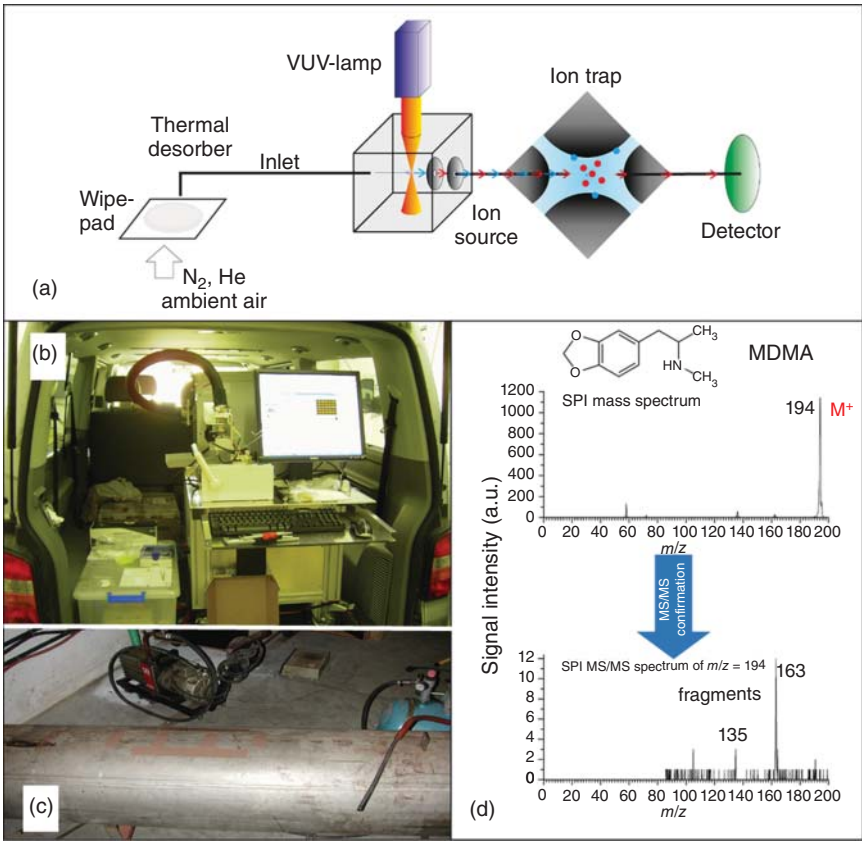

Figure 3.11 Application of a mobile photoionization ion trap mass spectrometer system (SPI-ITMS) for a real-scenario field test study in cooperation with the German Federal Police (BKA) for the detection of the illegal drug MDMA ("Ecstasy") at a clandestine MDMA laboratory. (a) Scheme of the SPI-ITMS system for wipe pad analysis (thermal desorption). (b) Photograph of the SPI-ITMS system with wipe pad desorber, mounted in a van for at-site measurements. (c) Photograph of the wipe pad sampling site (tube) during the onsite investigations. (d) SPI mass spectra depicting the molecular ion of MDMA, thermally desorbed from the wipe pad taken at the tube in (c) (top) and fragment ions of the simultaneous measured tandem mass spectrum (MS/MS) of the 194 m/z peak (bottom). The SPI-MS/MS fragment spectrum of the 194 m/z peak allows the validation of the assignment that MDMA residues were found on the tube in (c) in the former clandestine MDMA laboratory. Modified after (Schramm et al. 2009a). Reproduced (modified) with permission of Springer.

ionization is almost fragment free in this case and mainly intact molecular ions are obtained, SPI-MS provides an additional separation dimension. Substances that are not separated thoroughly on the GC-column and are coeluting could be distinguished by SPI-MS, if they have different molecular masses. In this vein, SPI-MS could be regarded as enhancing the separation space, distinguishing compounds according to their molecular mass. The hyphenated system of gas chromatography and SPI-MS could then be described as a comprehensive multi-dimensional analytical device similarly to two-dimensional gas chromatography,

albeit with different separation capabilities (Eschner et al. 2010; Welthagen et al. 2007).

The GC/SPI-MS coupling principle even works with hydrocarbon mixtures containing a larger number of constitutional and structural isomers, which can be separated by either gas chromatography retention time or molecular mass, respectively (Isaacman et al. 2012). This could be demonstrated with complex hydrocarbon matrices such as diesel fuel (Mitschke et al. 2006b) and even crude oil (Worton et al. 2015). The separation power could be augmented even further by adding a second chromatographic dimension, i.e. hyphenating two-dimensional comprehensive gas chromatography (GC × GC) with SPI-MS (Eschner et al. 2010; Eschner et al. 2011a; Worton et al. 2017). Figure 3.12 shows how the two-dimensional chromatographic GC × GC separation plane (Figure 3.12a) can be transferred in a three-dimensional separation space, if soft SPI ionization MS is established as further separation axis according to molecular mass (Figure 3.12c).

An apparent advantage of the GC/SPI-MS coupling is the enhancement of detection capability with respect to isobaric compounds, if a low-resolution mass spectrometer is used that could not distinguish between substances with the same nominal molecular mass. This becomes especially important, if a compound of interest or a known hazardous substance with adverse health effects has isobaric interferences. One example is cigarette smoke, where the toxic compounds butadiene and isoprene are isobaric to butyne and furan, respectively. Directing the exhaled smoke to a fast GC separation before the SPI-MS device allows to distinguish between these isobaric molecules with a time resolution of less than a minute. This enables a cigarette puff-resolved puff-by-puff analysis (Eschner et al. 2011a).

Another possible approach to support SPI-MS with respect to identification of chemical species is the parallel introduction of other ionization techniques that provide different information about the composition of gaseous mixtures. One obvious choice is electron ionization (EI), which enables substance identification by means of the characteristic fragmentation patterns. The combined EI/SPI ion source can be combined-again with gas chromatography (1D or 2D) but requires a fast switching between the two ionization methods (Eschner et al. 2011b). Another variant is the implementation of a filament and a VUV lamp to a linear ion trap (Wu et al. 2017). With both approaches, the identification of components from complex hydrocarbon mixtures such as diesel or gasoline profits from the complimentary information delivered from the different ionization schemes. This is depicted in Figure 3.12, where a GC × GC-SPI-ToFMS analysis with additional EI-MS spectra of a diesel sample is shown. Figure 3.12b,d depict simultaneously recorded SPI and EI mass spectra recorded during the GC × GC separation of a diesel fuel sample (Figure 3.12a), depicting the softness of the photo ionization method. This enables the separation of co-eluting compounds as shown in Figure 3.12d. Adding the soft ionization mass spectra to the two-dimensional retention time-based information yields a three-dimensional separation space of the diesel fuel (Figure 3.12c) constituents. Figure 3.10b demonstrates the gained additional separation power, where three coeluting compounds are distinguished by the different masses of their unfragmented

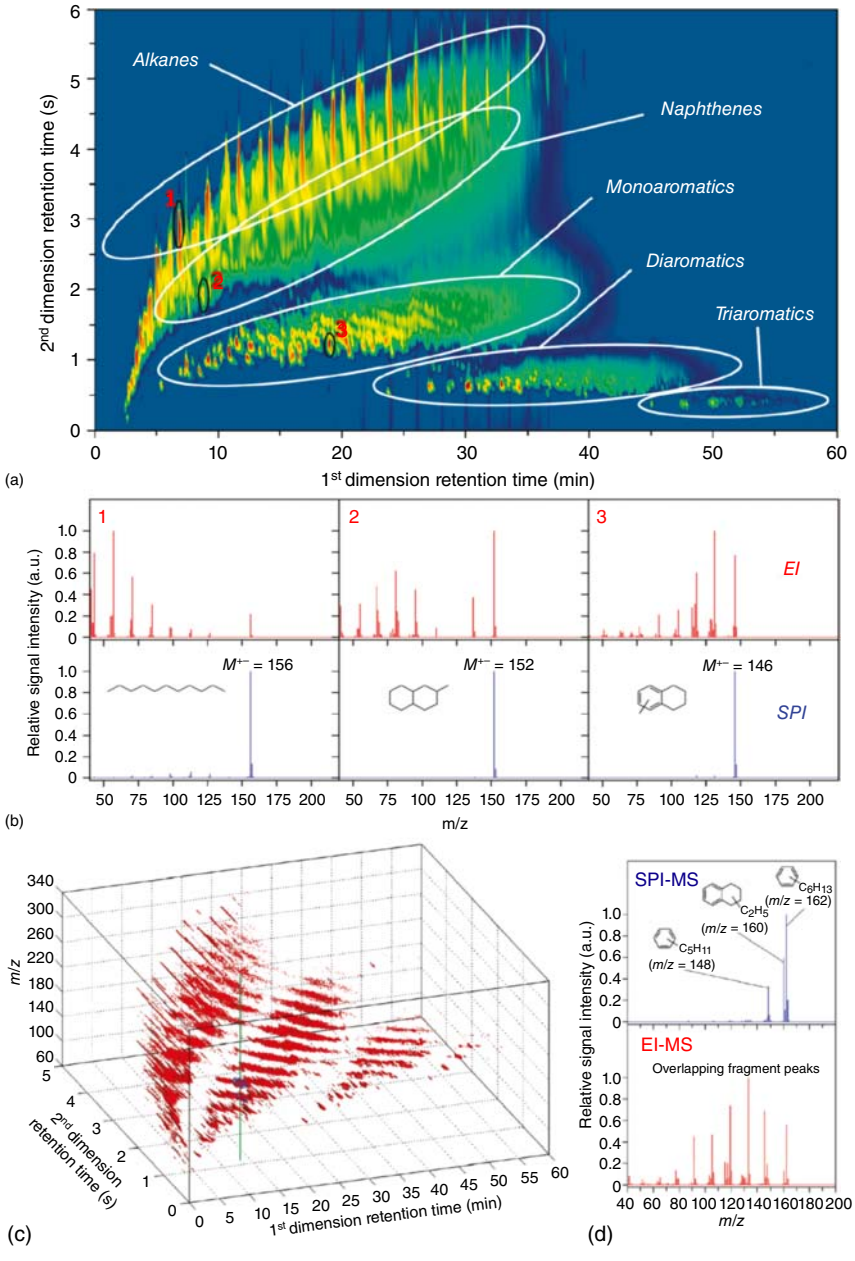

Figure 3.12 (a) Two-dimensional comprehensive gas chromatogram (GC × GC) of diesel fuel recorded by a GC × GC-SPI/EI-TOFMS instrument. For each pixel on the 2D-separation plane a SPI- as well as an EI-mass spectrum exists. (b) EI- and SPI-mass spectra of the peaks marked by 1, 2 and 3 in the separation plane (a), showing the EI-fragmantion pattern (red) or solely the respective molecular ion by soft SPI (blue). (c) The 3D volume plot of a GC × GC-SPI-ToFMS measurement, generated by plotting of the first- and second-dimension retention times against the molecular mass (third dimension), is displaying the most intense peaks of the GC × GC × MS data. The softness of SPI renders the mass axis as a further (molecular weight) separation dimension. (d) SPI-MS (blue) and EI-MS (red) spectra of overlapping peaks from the position marked by the green line in the (c) 3D volume plot, after Eschner et al. (2011b).

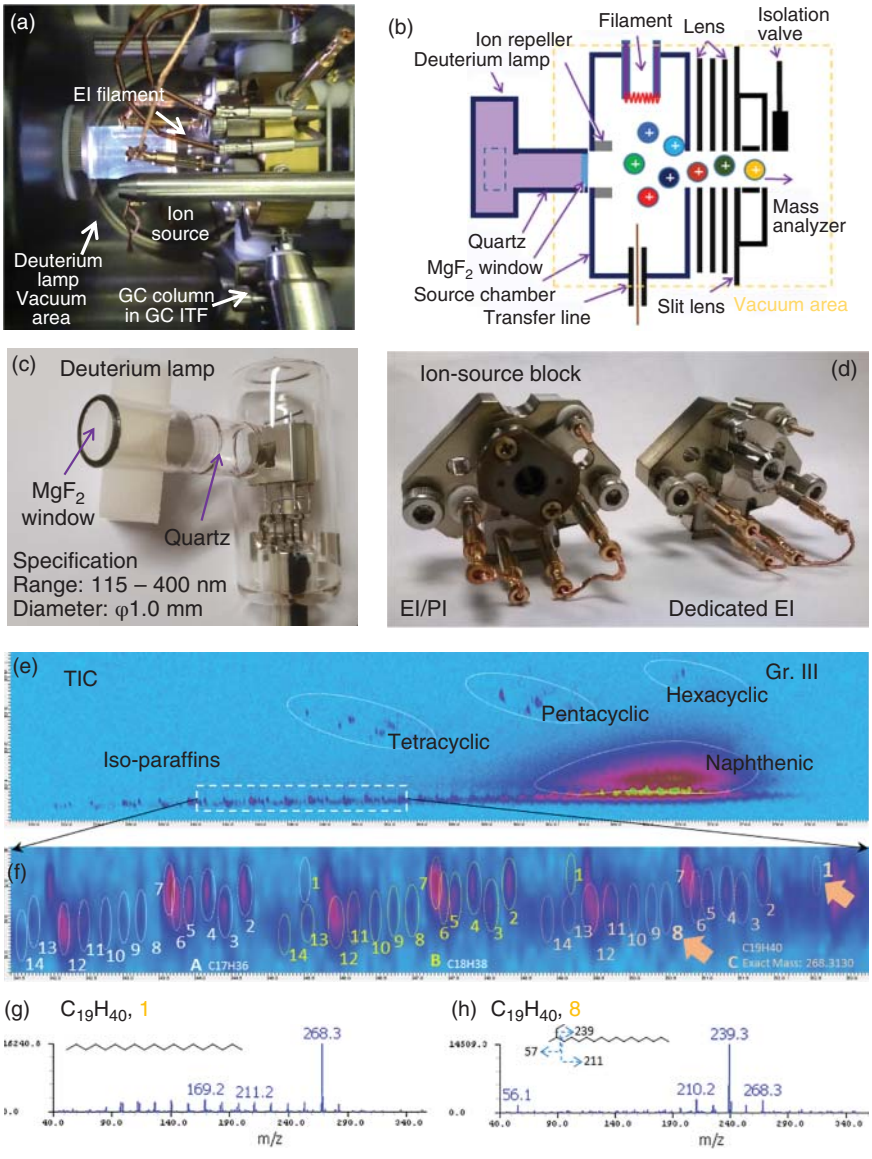

Figure 3.13 Integration of a deuterium lamp to a ToF ion source for SPI (Jeol AccuTOF). (a) Ion source with deuterium lamp and EI/SPI ion source block. The MgF_2 window of the deuterium lamp is placed very close to the ion source block. (b) Schematics of the EI/SPI ion source. The source could be operated either in EI or in SPI mode. (c) Applied deuterium lamp (commercially available from Hamamatsu Inc.). (d) Comparison between EI/SPI- and dedicated EI-ion source block of the system. (e) GC × GC-SPI-ToFMS of a base oil sample. (f) Isoparaffin pattern. (g) SPI spectrum of n-nonadecane (1, see arrow in (f)). (h) SPI spectrum of 2-ethylheptadecane (8, see arrow in (f)). Source: Modified and extended after Giri et al. (2017).

molecular ions. With EI-MS, such a differentiation is not possible because all compounds are fragmented into similar ions.

Another example is shown in Figure 3.13, depicting the integration of a deuterium lamp as VUV photon source to a GC × GC-ToFMS system (Giri et al. 2017). The ion source again can be operated either with EI or with SPI. The soft ionization method is able to cope well with complex samples such as oil or other petrochemical mixtures.

The basic approach of exploiting fragmentation to improve substance identification and at the same time having available the molecular ion pattern from SPI could also be reached by executing fragmentation with the help of collision-induced dissociation integrated in the SPI ion source (Hua et al. 2015). Such a device does not need the coupling of separation technologies or tandem-MS setups.

A combination of lamp-based SPI with chemical ionization (CI) is conceivable as well, with oxygen cations as the primary ions for CI (Hua et al. 2011).

Flow injection of liquid samples combined with SPI-MS under vacuum conditions is a preliminary step on the way to a full high performance liquid chromatography-single-photon ionization-mass spectrometry (HPLC-SPI-MS) coupling. Figure 3.14 displays the setup of such an ion source, in which VUV ionization is paired with electron ionization and coupled to a quadrupole mass spectrometer (Schepler et al. 2013). The eluent is introduced into the ionization region by a 25-µm-ID fused silica/PEEK capillary placed about 1 mm away from the heated repeller surface. After fast nebulization and desolvation of the droplets, the gas-phase molecules are ionized by EI or SPI and guided to the quadrupole MS.

The combination of the respective EI-MS and SPI-MS date positively reflects the complimentary benefit of carrying out both ionization methods for the same sample, as is shown in Figure 3.14b. With EI, the typical library fragmentation pattern for a compound is obtained, which serves as an identification scheme at least for the substance class of the respective compound. The SPI method clearly

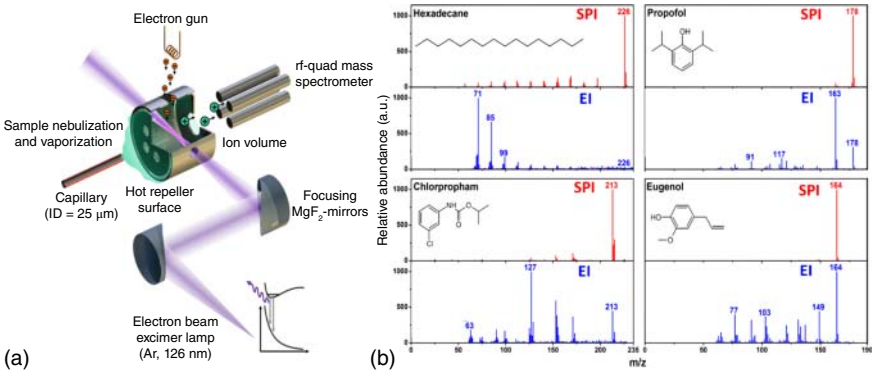

Figure 3.14 (a) Setup of a direct inlet for liquid samples with photoionization and electron ionization. (b) Corrected SPI (top) and EI (bottom) spectra and the respective NIST spectra (inset) for hexadecane, propofol, chlorpropham, and eugenol: the EI fragment mass spectra depict the fragmentation pattern in good agreement, whereas the SPI spectra are dominated by the molecular ions. Source: From Schepler et al. (2013).

carves out the molecular ion, which is helpful if it is hardly visible with EI or if a more complex mixture is investigated containing multiple representatives of the same substance class, yielding the same fragmentation patterns.

The SPI-MS approach, as an organic profiling and fingerprinting technology, obviously is a good candidate for hyphenation to thermal analysis. Thermal analysis is the general term for a family of analytical techniques, which are measuring the change of physical and chemical properties of samples as a function of temperature. In thermogravimetry (TG), the change of sample weight due to vaporization, pyrolytic decomposition, or reactions with gas-phase constituents is measured as a function of the temperature via an ultrasensitive microbalance. TG is often connected with EGA technologies such as mass spectrometry with EI (TG-MS) or Fourier transform infrared (TG-FTIR) spectroscopy. TG-MS is a particularly powerful technology for analysis of thermal decomposition products, e.g. providing information on the evolved small molecules such as CO, CO_2, NO, or CH_4. More complex organic molecules, however, are often not detectable intact because of fragmentation associated with EI. Thermal analysis-mass spectrometry (TA-MS) employing single-photon ionization allows the analysis of the evolved pattern of intact organic molecules and pyrolysis products in conjunction with thermal analysis data (weight loss and thermodynamic data if differential scanning calorimetry [DSC] is applied), and several systems have been developed (Arii and Otake 2008; Saraji-Bozorgzad et al. 2008). Figure 3.15a shows the setup of a coupling between a thermobalance and a SPI-ToFMS with an electron-beam pumped Ar excimer lamp as a VUV light source. Evaporated substances are guided through a heated interface and capillary transfer line. The mass spectrometer is working with orthogonal acceleration of the ions, enabling the recording of mass spectra with high frequencies from the continuous ion generation device. In the following, TG-SPI-MS measurement results on crude oils (Figure 3.15b) and on the simple polymer polyethylene (PE) as well as on two samples as a model for complex natural materials (Figure 3.16) are presented and briefly discussed exemplarily. Note that several applications of this technology on organic materials such as crude oils (Geissler et al. 2009), coal, further polymers, or biomass fractions (Streibel et al. 2009) have also been described.

Figure 3.15b gives an exemplary result from the TA-SPI-MS setup with capillary coupling, depicting the analysis of two crude oils. Appearance of evolved compounds is clearly distinguished into two different temperature zones. First, hydrocarbons evaporate corresponding to their respective boiling points. At higher temperatures, thermal decomposition (pyrolysis) of low-volatile substances begins, resulting in the horizontal band of pyrolysis products with lower molecular masses. This band describes the heavier fraction of the crude oil which either needs to be cracked for valorization or can used as heavy fuel oil/bitumen. Thus TG-SPI-MS allows a rather comprehensive analysis (i.e. the distillable and residual part) of heavy petrochemical fractions. By using a direct connection of the mass spectrometry to the thermal analysis, a nozzle-skimmer coupling, a sample transfer without wall contact is possible (Saraji-Bozorgzad et al. 2011; Varga et al. 2017). This is particular advantageous with respect to effective transfer of unstable species evolving from the thermobalance (TG device) as well as very effective in enhancing the detection sensitivity of compounds with

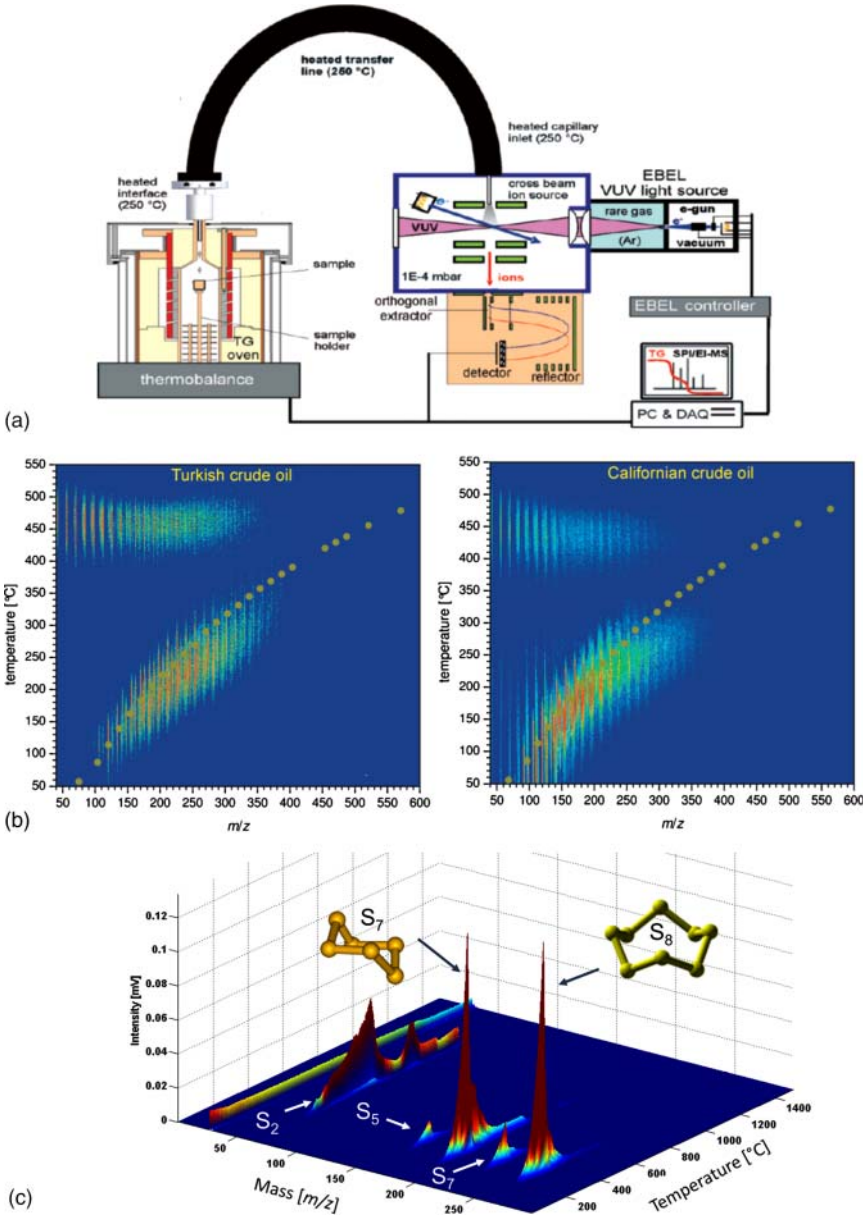

Figure 3.15 (a) Experimental setup of the hyphenated instrument between thermobalance and time-of-flight mass spectrometer with SPI beam source using a capillary coupling. (b) Contour plots of crude oil samples (Turkish crude oil and Californian crude oil) measured with the hyphenated instrument, depicting the appearance of evolved compounds as a function of oven temperature. Source: From Geissler et al. (2009). (c) A hyphenated instrument between a thermobalance and SPI time-of-flight mass spectrometer, using a skimmer coupling (Netzsch GmbH, Germany) for contact-less transfer to a ToFMS analyzer (PhotoTOF, Photonion GmbH, Germany), is used for analysis of sulfur clusters in sulfur vapor. Cyclic S_8 and S_6 are the most pronounced species, with S_8 being slightly higher abundant at lower temperatures. Smaller amounts of S_5 and S_6 are present, at higher temperatures S_2 dominates. Interestingly S_6 is more abundant (i.e. stable) than S_8 above 400 °C. Source: Unpublished data from authors. See also Varga et al. (2017) for similar measurements with a smaller temperature range.

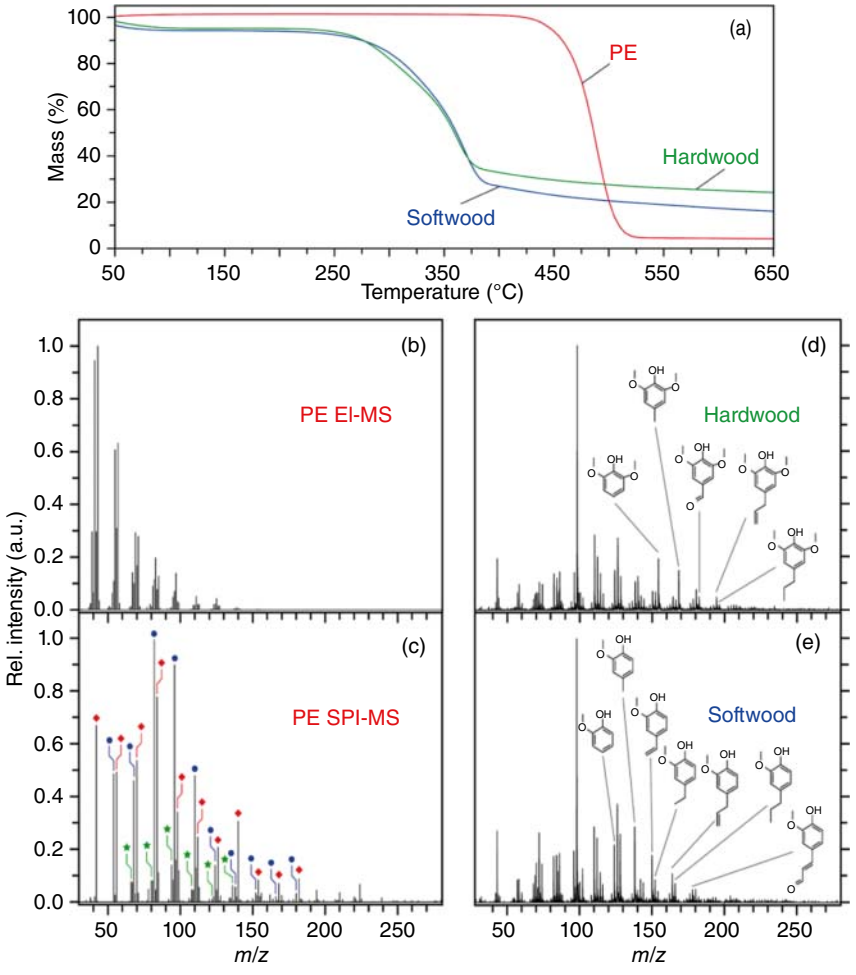

Figure 3.16 SPI-MS of evolved gas analysis (EGA) in thermal analysis (TA): results from a thermogravimetry – SPI-MS system (TG-SPI-MS), coupling of STA TA-device from Netzsch GmbH with a SPI-ToFMS system). A similar system is commercially available by Photonion GmbH (see Section 3.8). (a) Thermogravimetric curves, showing the weight loss of samples vs. temperature for polyethylene (PE), softwood, and hardwood. (b, c) Display an EI and SPI mass spectrum of PE, respectively. (d, e) Show a SPI mass spectrum of hardwood and softwood, respectively. Here, the focus lies on the indicated phenolic sinapyl- and guaiacyl-units (polyphenols), which are common marker substances for discrimination of hardwood and softwood. For further explanation, see text. Source: Unpublished data of the authors.

higher molecular masses. TG-skimmer devices can be coupled to quadrupole- or ToF-mass spectrometry. Figure 3.15c depicts a measurement of the molecular sulfur species in the gas phase using this technique (TG-skimmer-SPI-ToFMS coupling).

In Figure 3.16a, the thermogravimetric curves (TG curves) are depicted for hardwood (birch, green line), softwood (spruce, blue line), and polyethylene (PE, red line). The steep weight loss curve in the case of PE indicates that PE rapidly starts to decompose when a temperature of about 450 °C is reached exhibiting a maximal decomposition rate (i.e. volatilization rate) at 475 °C. The wood

samples, which in principle represent a complex biopolymeric composite of cellulose and hemicelluloses (polymeric carbohydrates) as well as lignin (polymeric polyphenol structure), exhibit a more gradual decomposition. However, in spruce (softwood), the lignin polymer is predominantly composed of guaiacyl units, and in birch, sinapyl units are also present. This leads to a higher thermal stability of the hardwood during the charring process. Below the TG curves, EGA mass spectra are shown in Figure 3.16b–e. The evolved gas analysis-electron ionization (EGA-EI) mass spectrum recorded at the highest decomposition rate of the PE measurement depicts typical fragments for unsaturated hydrocarbons (Figure 3.16b). The chemical information achievable, however, is limited because of the fragmentation inherently associated with EI. In contrary, the EGA mass spectrum recorded with soft electron beam pumped excimer lamp-single-photon ionization (EBEL-SPI) clearly depicts the molecular fingerprint of the homologous series of alkenes (◆), dienes (●), and trienes (★) evolving during the PE decomposition also at higher molecular masses, as indicated in Figure 3.16c and thus gives a good overview of the distribution of pyrolysis products of the decomposing polymer. In Figure 3.16d,e, the SPI mass spectra of the hardwood and softwood samples are shown. The mass spectra are characterized by decomposition products of cellulose (e.g. phenol derivatives) and lignin (e.g. carboxylic or furan compounds, the intense peak at 98 m/z in both mass spectra, e.g., is due to furfuryl alcohol). The SPI mass spectra mainly differ in the more pronounced signals deriving from the sinapyl units of the lignin polymer in the case of birch wood. In summary, the coupling of thermal analysis (TA) methods to SPI mass spectrometry allows a fast characterization of evolved organic compounds. For the detection of trace compounds and the separation of isobaric compounds, a fast gas chromatographic step can be inserted between the TA and the SPI-MS system (Fischer et al. 2015; Saraji-Bozorgzad et al. 2010; Wohlfahrt et al. 2016).

Coupling of a thermobalance with a quadrupole mass spectrometer equipped with a VUV lamp for SPI is also possible. A scheme of a TG-skimmer-quadrupole

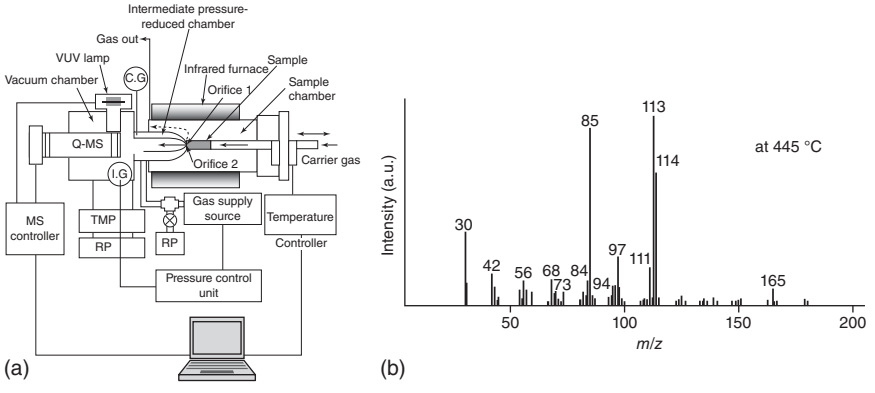

Figure 3.17 (a) Schematic diagram of a hyphenation between thermobalance and mass spectrometry using a skimmer interface system. I.G: ion gauge, C.G: crystal gauge, TMP: turbo molecular pump, RP: rotary pump. (b) Mass spectrum for the evolved gas analysis coupled with photoionization mass spectrometry via a skimmer coupling for a Nylon-6 sample recorded at maximum TIC peak temperature of 445 °C. TIC, total ion current. Source: From Arii and Otake (2008).

mass spectrometry hyphenation's setup is shown in Figure 3.17a (Arii and Otake 2008). A similar system is commercialized by Rigaku (see section 3.8). Quadrupole mass spectrometers (QMS) systems are cheaper than ToF mass analyzers but are exhibiting a reduced sensitivity, measurement speed and mass range. However, many TG-SPI-MS applications, such as the Nylon-6 pyrolysis depicted in Figure 3.17b, can be also addressed well by QMS systems. The higher data acquisition rate of TG-skimmer-ToFMS is demonstrated in the sulfur application depicted in Figure 3.15c.

The use of fast gas chromatography with rapid heating and short columns between thermobalance and SPI mass spectrometer could enhance the selectivity considerably. Recently an ultra-fast GC setup, using an optical heating by a halogen lamp and and fast air cooling was realized and applied for TG-fast GC-SPI-ToFMS analysis of food roasting processes (coffee, nuts; see Fischer et al. 2015, Fischer et al. 2017).

Specialized applications for some research areas are also available. Particulate matter from emission sources such as vehicles or wood combustion but also ambient aerosols sampled on quartz fiber filters are exposed to thermal desorption to release the organic content on the particles to the gas phase. The evolving molecules are then guided to a mass spectrometer with SPI ion source (Diab et al. 2015; Grabowsky et al. 2011).

Thermal desorption can also be utilized for the analysis of volatile organic species in water. The organic compounds are extracted by stir bar sorptive extraction, and the bar is then placed in a heating block. The evolving molecules are guided to the mass spectrometer equipped with a VUV source for SPI (Cui et al. 2012).

3.7 Ambient Monitoring

Ambient measurements require portable mass spectrometer solutions. Such a compact system based on SPI has been described in Gao et al. (2013). Its dimensions are 30 cm × 20 cm × 20 cm and its weight amounts to 15 kg. The device is powered by a lithium ion battery allowing three hours of operation. Ambient gas samples are introduced via a polydimethylsiloxane membrane inlet system, which enriches volatile organic compounds yielding improved limits of detection. VUV light (10.6 eV) for the ionization is generated by a commercial krypton lamp. A miniature reflectron ToF analyzer with a mass resolution of 450 at 106 m/z detects the molecular ions. Limits of detection of toluene and xylene can achieve 0.5 ppb and 0.4 ppb for one second measurement with a scan frequency of 10 kHz, respectively. Figure 3.18a contains a scheme of the system, which has been commercialized by the company Hexin Ltd. (see Section 3.8) and was applied for the sequential analysis of dimethyl sulfide (DMS) in surface seawater and air during a research cruise in western Antarctica (Zhang et al. 2019). The MI-SPI-TOFMS unit was coupled to an automatic sea water purge-and-trap system as well as to an air enrichment/desorption system. Every 10 minute the system alternatingly injects a desorption gas pulse from the air sampling/enrichment unit and a desorption gas pulse from the water purge-and-trap system sampling system to the MI-SPI-TOFMS detector.

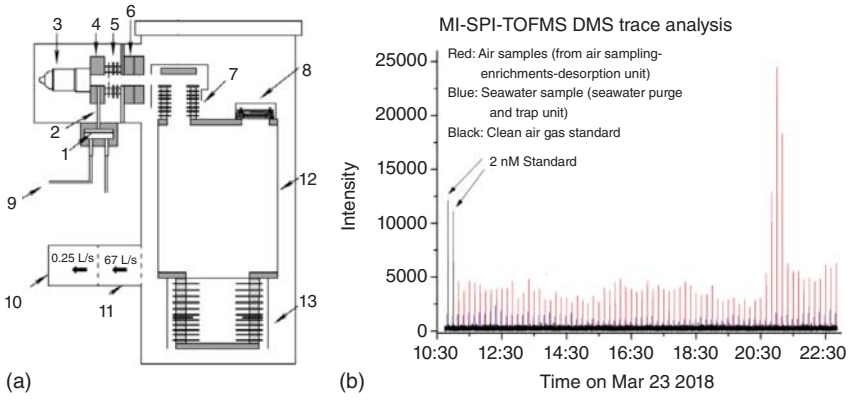

Figure 3.18 Portable mass spectrometer with a membrane inlet system and a VUV ionization time-of-flight mass spectrometer (Zhang et al. 2019). (a) Setup of the MS system 1. PDMS membrane injector, 2. Injector tube, 3. VUV lamp, 4. Ionization chamber, 5. Derivation electrode, 6. Einzel lens, 7. Ion acceleration region, 8. Ion detector, 9. Air sample inlet, 10. Micro-vacuum pump, 11. Mechanical pump, 12. Field-free drift tube, 13. Ion reflector. (b) Sequential measurement of dimethyl sulfide (DMS) in surface seawater and air by using water and air enrichment systems. Source: Zhang et al. (2019). Reproduced with permission of Elsevier.

Figure 3.18b shows a corresponding measurement trace of dimethyl sulfide in surface seawater (red peaks) and air (blue peaks).

3.8 Commercial Solutions

SPI-MS instruments are available from different instrument suppliers as stand-alone gas analyzers or hyphenated instruments. JEOL Ltd. Tokyo, Japan (www.jeol.co.jp/en/) offers photoionization sources for their gas chromatography–mass spectrometry systems as an alternative soft ionization approach to the commonly used electron ionization (see Section 3.6). A high-power deuterium lamp is utilized as the VUV beam source. The Rigaku Corporation from Tokyo (www.rigaku.com/en) has a coupled instrument connecting thermal analysis and quadrupole mass spectrometry (QMS) in their portfolio, which combines both electron ionization and photoionization with a VUV lamp. Also a skimmer coupling between TA and QMS is available, as depicted in Section 3.6. The Hexin company of Guangzhou, China (http://www.tofms.net/en/), offers lamp-based SPI Systems with membrane inlet to monitor organic gases and volatile industry chemicals in ambient air (as described in Section 3.7). Photonion GmbH from Schwerin, Germany (www.photonion.de), develops and markets customized time-of-flight mass spectrometer gas analyzers with different SPI ion sources, containing both lamp- and laser-based options for VUV beam generation and simultaneous operable other ion sources (electron ionization and resonance-enhanced multiphoton ionization). The systems are offered as stand-alone industrial process gas analyzers or hyphenated, e.g. to thermal analysis, smoking machines (for cigarettes, e-cigarettes, and other smoking products), gas chromatography, or aerosol filter carbon analyzers.

References

Adam, T. and Zimmermann, R. (2007). Determination of single photon ionization cross sections for quantitative analysis of complex organic mixtures. *Anal. Bioanal. Chem.* 389: 1941–1951.

Adam, T., Mitschke, S., Streibel, T. et al. (2006). Puff-by-puff resolved characterisation of cigarette mainstream smoke by single photon ionisation (SPI)-time-of-flight mass spectrometry (TOFMS): comparison of the 2R4F research cigarette and pure Burley, Virginia, Oriental and Maryland tobacco cigarettes. *Anal. Chim. Acta* 572: 219–229.

Al-Basheer, W., Hedén, M., Cai, Z.J., and Shi, Y.J. (2011). Study of two-photon resonant four-wave sum mixing in xenon in the spectral region of 105–110 nm. *Chem. Phys.* 381: 59–66.

Arii, T. and Otake, S. (2008). Study on thermal decomposition of polymers by evolved gas analysis using photoionization mass spectrometry (EGA-PIMS). *J. Therm. Anal. Calorim.* 91: 419–426.

Bauer, D. (2004). Small rare gas clusters in laser fields: ionization and absorption at long and short laser wavelengths. *J. Phys. B* 37: 3085–3101.

Chen, M.-C., Gerrity, M.R., Backus, S. et al. (2009). Spatially coherent, phase matched, high-order harmonic EVU beams at 50 kHz. *Opt. Express* 17: 17376–17383.

Couch, D.E., Buckingham, G.T., Baraban, J.H. et al. (2017). Tabletop femtosecond VUV photoionization and PEPICO detection of microreactor pyrolysis products. *J. Phys. Chem. A* 121: 5280–5289.

Cui, H., Hua, L., Hua, K. et al. (2012). Coupling of stir bar sorptive extraction with single photon ionization mass spectrometry for determination of volatile organic compounds in water. *Analyst* 137: 513–518.

Czech, H., Sippula, O., Kortelainen, M. et al. (2016a). On-line analysis of organic emissions from residential wood combustion with single-photon ionisation time-of-flight mass spectrometry (SPI-TOFMS). *Fuel* 177: 334–342.

Czech, H., Schepler, C., Klingbeil, S. et al. (2016b). Resolving coffee roasting-degree phases based on the analysis of volatile compounds in the roasting off-gas by photoionization time-of-flight mass spectrometry (PI-TOFMS) and statistical data analysis: toward a PI-TOFMS roasting model. *J. Agric. Food. Chem.* 64: 5223–5231.

Czech, H., Heide, J., Ehlert, S. et al. (2020). Smart online coffee roasting process control: modelling coffee roast degree and brew antioxidant capacity for real-time prediction by resonance-enhanced multi-photon ionization mass spectrometric (REMPI-TOFMS) monitoring of roast gases. *Foods* 9 (5).

Di Palma, T.M., Prati, M.V., and Borghese, A. (2009). Tunable single-photon ionization TOF mass spectrometry using laser-produced plasma as the table-top VUV light source. *J. Am. Soc. Mass Spectrom.* 20: 2192–2198.

Diab, J., Streibel, T., Cavalli, F. et al. (2015). Hyphenation of a EC/OC thermal-optical carbon analyzer to photo-ionization time-of-flight mass spectrometry: an off-line aerosol mass spectrometric approach for characterization of primary and secondary particulate matter. *Atmos. Meas. Tech.* 8: 3337–3353.

Dorfner, R., Ferge, T., Yeretzian, C. et al. (2004). Laser mass spectrometry as on-line sensor for industrial process analysis: process control of coffee roasting. *Anal. Chem.* 76: 1386–1402.

Eschner, M.S., Welthagen, W., Groeger, T.M. et al. (2010). Comprehensive multidimensional separation methods by hyphenation of single-photon ionization time-of-flight mass spectrometry (SPI-TOF-MS) with GC and GC × GC. *Anal. Bioanal.Chem.* 398: 1435–1445.

Eschner, M., Selmani, I., Gröger, T., and Zimmermann, R. (2011a). On-line comprehensive two-dimensional characterization of puff-by-puff resolved cigarette smoke by hyphenation of fast gas chromatography to single-photon ionization time-of-flight mass spectrometry: quantification of hazardous volatile organic compounds. *Anal. Chem.* 83: 6619–6627.

Eschner, M.S., Groeger, T.M., Horvath, T. et al. (2011b). Quasi-simultaneous acquisition of hard electron ionization and soft single-photon ionization mass spectra during GC/MS analysis by rapid switching between both ionization methods: analytical concept, setup, and application on diesel fuel. *Anal. Chem.* 83: 3865–3872.

Fendt, A., Streibel, T., Sklorz, M. et al. (2012). On-line process analysis of biomass flash pyrolysis gases enabled by soft photoionization mass spectrometry. *Energy Fuels* 26: 701–711.

Fischer, M., Wohlfahrt, S., Varga, J. et al. (2015). Optically heated ultra-fast-cycling gas chromatography module for rapid separation of direct sampling and online monitoring applications. *Anal. Chem.* 87: 8634–8639.

Fischer, M., Wohlfahrt, S., Varga, J., et al. (2017). Evolution of volatile flavor compounds during roasting of nut seeds by thermogravimetry coupled to fast-cycling optical heating gas chromatography-mass spectrometry with electron and photoionization. *Food Anal. Methods* 10(1): 49–62.

Gao, W., Tan, G., Hong, Y. et al. (2013). Development of portable single photon ionization time-of-flight mass spectrometer combined with membrane inlet. *Int. J. Mass spectrom.* 334: 8–12.

Geissler, R., Saraji-Bozorgzad, M.R., Groeger, T. et al. (2009). Single photon ionization orthogonal acceleration time-of-flight mass spectrometry and resonance enhanced multiphoton ionization time-of-flight mass spectrometry for evolved gas analysis in thermogravimetry: comparative analysis of crude oils. *Anal. Chem.* 81: 6038–6048.

Giri, A., Coutriade, M., Racaud, A. et al. (2017). Molecular characterization of volatiles and petrochemical base oils by photo-ionization GC × GC-TOF-MS. *Anal. Chem.* 89: 5395–5403.

Grabowsky, J., Streibel, T., Sklorz, M. et al. (2011). Hyphenation of a carbon analyzer to photo-ionization mass spectrometry to unravel the organic composition of particulate matter on a molecular level. *Anal. Bioanal. Chem.* 401(10): 3153–3164.

Hanna, S.J., Campuzano-Jost, P., Simpson, E.A. et al. (2009). A new broadly tunable (7.4–10.2 eV) laser based VUV light source and its first application to aerosol mass spectrometry. *Int. J. Mass spectrom.* 279: 134–146.

Heide, J., Czech, H., Ehlert, S. et al. (2020). Toward smart online coffee roasting process control: feasibility of real-time prediction of coffee roast degree and brew

antioxidant capacity by single-photon ionization mass spectrometric monitoring of roast gases. *J. Agric. Food Chem.* 68(17): 4752–4759.

Hertz-Schünemann, R., Streibel, T., Ehlert, S., and Zimmermann, R. (2013). Looking into individual coffee beans during the roasting process: direct micro-probe sampling on-line photo-ionisation mass spectrometric analysis of coffee roasting gases. *Anal. Bioanal.Chem.* 405: 7083–7096.

Hertz-Schünemann, R., Ehlert, S., Streibel, T. et al. (2015). High-resolution time and spatial imaging of tobacco and its pyrolysis products during a cigarette puff by microprobe sampling photoionisation mass spectrometry. *Anal. Bioanal.Chem.* 407: 2293–2299.

Horio, T., Spesyvtsev, R., and Suzuki, T. (2014). Generation of sub-17 fs vacuum ultraviolet pulses at 133 nm using cascaded four-wave mixing through filamentation in Ne. *Opt. Lett.* 39: 6021–6024.

Hua, L., Wu, Q., Hou, K. et al. (2011). Single photon ionization and chemical ionization combined ion source based on a vacuum ultraviolet lamp for orthogonal acceleration time-of-flight mass spectrometry. *Anal. Chem.* 83: 5309–5316.

Hua, L., Hou, K., Chen, P. et al. (2015). Realization of in-source collision-induced dissociation in single-photon ionization time-of-flight mass spectrometry and its application for differentiation of isobaric compounds. *Anal. Chem.* 87: 2427–2433.

Isaacman, G., Wilson, K.R., Chan, A.W.H. et al. (2012). Improved resolution of hydrocarbon structures and constitutional isomers in complex mixtures using gas chromatography-vacuum ultraviolet-mass spectrometry. *Anal. Chem.* 84: 2335–2342.

Jia, L., Le-Brech, Y., Shrestra, B. et al. (2015). Fast pyrolysis in a microfluidized bed reactor: effect of biomass properties and operating conditions on volatiles composition as analyzed by online single photoionization mass spectrometry. *Energy Fuels* 29: 7364–7374.

Kleeblatt, J., Schubert, J.K., and Zimmermann, R. (2015). Detection of gaseous compounds by needle trap sampling and direct thermal-desorption photoionization mass spectrometry: concept and demonstrative application to breath gas analysis. *Anal. Chem.* 87: 1773–1781.

Kuribayashi, S., Yamakoshi, H., Danno, M. et al. (2005). VUV single-photon ionization ion trap time-of-flight Mass spectrometer for on-line, real-time monitoring of chlorinated organic compounds in waste incineration flue gas. *Anal. Chem.* 77: 1007–1012.

Liu, W., Jiang, J., Hou, K. et al. (2016). Online monitoring of trace chlorinated benzenes in flue gas of municipal solid waste incinerator by windowless VUV lamp single photon ionization TOFMS coupled with automatic enrichment system. *Talanta* 161: 693–699.

Mitschke, S., Adam, T., Streibel, T. et al. (2006a). Application of time-of-flight mass spectrometry with laser-based photo-ionization methods for time-resolved on-line analysis of mainstream cigarette smoke. *Anal. Chem.* 77: 2288–2296.

Mitschke, S., Welthagen, W., and Zimmermann, R. (2006b). Comprehensive gas chromatography-time-of-flight mass spectrometry using soft and selective photoionization techniques. *Anal. Chem.* 78: 6364–6375.

Morozov, A., Heindl, T., Krücken, R., et al. (2008). Conversion efficiencies of electron beam energy to vacuum ultraviolet light for Ne, Ar, Kr, and Xe excited with continuous electron beams. *J. Appl. Phys* 103: 103301. https://doi.org/10.1063/1.2931000.

Mühlberger, F., Wieser, J., Ulrich, A. et al. (2002). Single photon ionization (SPI) via incoherent VUV-excimer light: Robust and compact time-of-flight mass spectrometer for on-line, real-time process gas analysis. *Anal. Chem.* 74: 3790–3801.

Mullen, C., Irwin, A., Pond, B.V. et al. (2006). Detection of explosives and explosives-related compounds by single photon laser ionization time-of-flight mass spectrometry. *Anal. Chem.* 78: 3807–3814.

Popmintchev, D., Hernández-García, C., Dollar, F. et al. (2015). Ultraviolet surprise: efficient soft X-ray high-harmonic generation in multiply ionized plasmas. *Science* 350: 1225–1231.

Qi, F. (2013). Combustion chemistry probed by synchrotron VUV photoionization mass spectrometry. *Proc. Combust. Inst.* 34: 33–63.

Qi, F., Yang, R., Yang, B. et al. (2006). Isomeric identification of polycyclic aromatic hydrocarbons formed in combustion with tunable vacuum ultraviolet photoionization. *Rev. Sci. Instrum.* 77: 84101.

Ren'an, B., Mingdong, S., Zhongrui, W. et al. (2012). Development of 146 nm vacuum UV light source. *Physics Procedia* 32: 477–481.

Salvermoser, M. and Murnick, D.E. (2004). Stable high brightness radio frequency driven micro-discharge lamps at 193 (ArF*) and 157 nm (F_2*). *J. Phys. D: Appl. Phys.* 37: 180–184.

Saraji-Bozorgzad, M., Geißler, R., Streibel, T. et al. (2008). Thermogravimetry coupled to single photon ionization quadrupole mass spectrometry: a novel tool to investigate the chemical signature of thermal decomposition of polymeric materials. *Anal. Chem.* 80: 3393–3403.

Saraji-Bozorgzad, M.R., Eschner, M., Groeger, T.M. et al. (2010). Highly resolved online organic-chemical speciation of evolved gases from thermal analysis devices by cryogenically modulated fast gas chromatography coupled to single photon ionization mass spectrometry. *Anal. Chem.* 82: 9644–9653.

Saraji-Bozorgzad, M.R., Streibel, T., Kaisersberger, E. et al. (2011). Detection of organic products of polymer pyrolysis by thermogravimetry-supersonic jet-skimmer time-of-flight mass spectrometry (TG-Skimmer-SPI-TOFMS) using an electron beam pumped rare gas excimer VUV-light source (EBEL) for soft photo ionisation. *J. Therm. Anal. Calorim.* 105: 691–697.

Sato, R., Yasumatsu, D., Kumagai, S. et al. (2014). An atmospheric pressure inductively coupled microplasma source of vacuum ultraviolet light. *Sens. Actuators, A* 215: 144–149.

Schepler, C., Sklorz, M., Passig, J. et al. (2013). Flow injection of liquid samples to a mass spectrometer with ionization under vacuum conditions: a combined ion source for single-photon and electron impact ionization. *Anal. Bioanal.Chem.* 405: 6953–6957.

Schramm, E., Hölzer, J., Pütz, M., et al. (2009a). Real-time trace detection of security-relevant compounds in complex sample matrices by thermal

desorption-single photon ionization-ion trap mass spectrometry (TD-SPI-ITMS). *Anal. Bioanal. Chem.* 395: 1795–1807.

Schramm, E., Kürten, A., Hölzer, J., et al. (2009b). Trace detection of organic compounds in complex sample matrixes by single photon ionization ion trap mass spectrometry: real-time detection of security-relevant compounds and online analysis of the coffee-roasting process. *Anal. Chem.* 81: 4456–4467.

Streibel, T., Geißler, R., Saraji-Bozorgzad, M. et al. (2009). Evolved gas analysis (EGA) in TG and DSC with single photon ionisation mass spectrometry (SPI-MS): molecular organic signatures from pyrolysis of soft and hard wood, coal, crude oil and ABS polymer. *J. Therm. Anal. Calorim.* 96: 795–804.

Ubachs, W., Salumbides, E.J., Eikema, K.S.E. et al. (2014). Novel techniques in VUV high-resolution spectroscopy. *J. Electron. Spectrosc. Relat. Phenom.* 196: 159–164.

Varga, J., Wohlfahrt, S., Fischer, M. et al. (2017). An evolved gas analysis method for the characterization of sulfur vapor. *J. Therm. Anal. Calorim.* 127: 955–960.

Wang, D., Li, W., Ding, L., and Zeng, H. (2014). Enhanced XUV pulse generation at 89 nm via nonlinear interaction of UV femtosecond filaments. *Opt. Lett.* 39: 4140–4143.

Wang, Y., Huang, Q., Zhou, Z. et al. (2015). Online study on the pyrolysis of polypropylene over the HZSM-5 zeolite with photoionization time-of-flight mass spectrometry. *Energy Fuels* 29: 1090–1098.

Wang, Y., Jiang, J., Huo, K. et al. (2016). High-pressure photon ionization source for TOFMS and its application for online breath analysis. *Anal. Chem.* 88: 9047–9055.

Welthagen, W., Mitschke, S., Mühlberger, F., and Zimmermann, R. (2007). One-dimensional and comprehensive two-dimensional gas chromatography coupled to soft photo ionization time-of-flight mass spectrometry: a two- and three-dimensional separation approach. *J. Chromatogr. A* 1150: 54–61.

Wohlfahrt, S., Fischer, M., Varga, J. et al. (2016). Dual-stage consumable-free thermal modulator for the hyphenation of thermal analysis, gas chromatography, and mass spectrometry. *Anal. Chem.* 88: 640–644.

Worton, D.R., Zhang, H., Isaacman-VanWertz, G. et al. (2015). Comprehensive chemical characterization of hydrocarbons in NIST standard reference material 2779 Gulf of Mexico crude oil. *Environ. Sci. Technol.* 49: 13130–13138.

Worton, D.R., Decker, M., Isaacman-VanWertz, G. et al. (2017). Improved molecular level identification of organic compounds using comprehensive two-dimensional chromatography, dual ionization energies and high resolution mass spectrometry. *Analyst* 142: 2395–2403.

Wu, Q., Tian, Y., Li, A. et al. (2017). A miniaturized linear wire ion trap with electron ionization and single photon ionization sources. *J. Am. Soc. Mass. Spectrom.* 28: 859–865.

Xu, J., Zhuo, J., Zhu, Y. et al. (2017). Analysis of volatile organic pyrolysis products of bituminous and anthracite coals with single-photon ionization time-of-flight mass spectrometry and gas chromatography/mass spectrometry. *Energy Fuels* 31: 730–737.

Yamamoto, Y., Kambe, Y., Yamada, H., and Tonokura, K. (2012). Measurement of volatile organic compounds in vehicle exhaust using single-photon ionization time-of-flight mass spectrometry. *Anal. Sci.* 28: 385–390.

Yin, S. and Bernstein, E.R. (2012). Gas phase chemistry of neutral metal clusters: distribution, reactivity and catalysis. *Int. J. Mass spectrom.* 321–322: 49–65.

Zhang, Y., Sun, W., Shang, D., et al. (2017). Investigation on the influence of time-of-day on benzene metabolic pharmacokinetics by direct breath analysis in mice. *Chemosphere* 184: 93–98.

Zhang, M., Gao, W., Yan, J., et al. (2019). An integrated sampler for shipboard underway measurement of dimethyl sulfide in surface seawater and air. *Atmos. Envirom.* 209: 86–91.

Zhu, Z., Wang, J., Qiu, K. et al. (2014). Note: a novel vacuum ultraviolet light source assembly with aluminum-coated electrodes for enhancing the ionization efficiency of photoionization mass spectrometry. *Rev. Sci. Instrum.* 85: 46110.

Zimmermann, R., Hertz-Schünemann, R., Ehlert, S. et al. (2015). Highly time-resolved imaging of combustion and pyrolysis product concentrations in solid fuel combustion: NO formation in a burning cigarette. *Anal. Chem.* 87: 1711–1717.